Ecole Nationale des Ponts et Chaussées

2017-2018

Projet de Fin d'Etudes

Département Génie Civil et Construction

Stefania THEODOROU

Ingénieur élève double diplôme

Tuteur professionnel : Elisabeth PALIX

Tuteur académique : Jean-Michel PEREIRA

Modèle sol-structure pour le dimensionnement des monopieux offshore

Soil-Structure model for the design of offshore monopiles

Projet réalisé au sein de EDF Energies Nouvelles
Cœur Défense - Tour B
100, esplanade du Général de Gaulle
92932 Paris La Défense Cedex

19/2/2018-10/08/2018

Remerciements

Tout d'abord, j'adresse mes remerciements à Mme Elisabeth PALIX, mon maître de stage et ingénieurgéotechnique réfèrent d' EDF Energies Nouvelles, pour son encadrement et l'intérêt versé dans ma formation pendant les 6 mois de mon stage. Je tiens à la remercier vivementpour son accueil, le temps passé ensemble et le partage de son expertise au quotidien. Sa contribution était significative pour le développement de mes compétences techniques et scientifiques. Grâce à sa confiance j'ai pu m'accomplir totalement dans mes missions.

Je tiens aussi à remercier M Jean Michel PEREIRA, mon tuteur académique et professeur à l'Ecole des Ponts et Chaussées, pour son encouragement généreux et son aide cruciale sur le choix de ce PFE ainsi que sur sa réalisation tout au long de mon stage.

Je remercie également Mme Pascale De MUYNCK (Responsable Ingénierie Civile) de m'avoir offert l'opportunité d'intégrer l' équipe offshore d' EDF EN.

Je remercie finalement toute l'équipe EDF EN pour leur accueil au sein de l'entreprise, leur énergie et leur esprit d'équipe au travail.

Résumé

L'objectif de ce projet de fin d'études est de développer un module géotechnique dans un logiciel de prédimensionnement de monopieux développé par EDF R&D. EDF EN a mandaté EDF R&D pour développer un outil qui permettra de réaliser un dimensionnement complet d'un monopieu en phase conceptuelle d'un projet. EDF EN a eu à charge de fournir le module sol. Les modèles d'interaction sol structure proposés dans les standards actuels sont essentiellement basés sur l'expérience Oil&Gaz et ne sont pas adaptés aux défis des fondations d'éoliennes en mer (large diamètre, nombre de cycle de chargement très important etc). Plusieurs projets de recherche ont été réalisés ou sont en cours de réalisation afin d'améliorer la prise en compte de l'interaction sol-structure dans le dimensionnement des monopieux. On peut notamment citer le projet PISA qui réunit les principaux acteurs du secteur (dont EDF EN) et le projet SOLCYP où EDF EN a participé, qui permet de prendre en compte le nombre des cycles lors du chargement cyclique. Afin de profiter de l'optimisation rendue possible par ces travaux de recherche, EDF EN souhaitait implémenter leurs résultats (méthodes proposées) dans le module sol à développer. Le travail consistait dans un premier temps à se familiariser avec les travaux de recherche auxquels EDF EN a participé et ceux disponibles dans la littérature. Ensuite, il faudrait définir le cahier des charges du module sol afin qu'il soit facilement intégré au logiciel plus global développé par EDF R&D. La dernière partie du stage consistait à définir le processus de validation du module et le tester sur des cas réels.

Mots-clés : géotechnique, offshore, monopieu, predimensionnement, latéral, cyclique, interaction, logiciel

Abstract

The aim of this master thesis is to develop a geotechnical module in a predesign software for monopiles developed by EDF R&D. EDF EN has commissioned EDF R&D to create a tool that will make it possible to carry out a complete dimensioning of a monopile in the conceptual phase of a project and EDF EN is responsible for providing the soil module. The soil structure interaction models proposed in the current standards are essentially based on the Oil & Gas experience and are not adapted to the particularities of offshore wind turbine foundations (large diameter, very large number of loading cycles etc.). Several research projects have been carried out or are underway to improve the consideration of soil-structure interaction in the design of monopiles. For example, the PISA project that brings together the main players in the sector (including EDF EN) and the SOLCYP project in which EEDF EN was involved, which takes into account the number of cycles during cyclic loading. In order to take advantage of the optimization made possible by this research work, EDF EN wanted to implement their results (proposed methods) in the soil module to be developed. The work initially consisted in getting familiar with the research work in which EDF EN participated and with the related literature. Then, the specifications of the soil module should be defined so that it can be easily integrated into the global software developed by EDF R&D. The last part of the internship was to define the validation process of the module and test it on real cases.

Keywords: geotechnics, offshore, monopile, predesign, lateral, cyclic, interaction, software

Summary

List of tables

List of figures

List of abbreviations

API		American Petroleum Institut
RP		Recommended Practise
DNV		Det Norske Veritas
PISA		PIle Soil Analysis
SOLCYP		SOLicitation CYclique de Pieux
FLS		Fatigue Limit State
ULS		Ultimate Limit State
SLS		Serviceability Limit State
NFA		Natural Frequency Analysis
γ_f		Load factor
γ_M		Material factor
N_{SLS}	-	Number of cycles at SLS
N_{ULS}	-	Number of cycles at ULS
N_{NFA}	-	Number of cycles at NFA
N_{FLS}	-	Number of cycles at FLS
FE	-	Finite Element analysis
L	m	Pile length
L_{crit}	m	Critical pile length
θ_{perm}	°	Permanent pile head rotation
E_p	Pa	Modulus of elasticity of the pile
I_p	m^4	Moment of inertia of the pile
γ'	N/m^3	Effective unit weight of soil
k_{p-y}	Pa/m	Coefficient of horizontal soil resistance
S_u	Pa	undrained shear strength
D	m	pile diameter at depth z

σ'_v	Pa	effective vertical stress at depth z
y_{50}	m	Deflection at 50% maximum stress
p	N/m	Lateral soil reaction
E_{50}	-	Strain at 50% maximum stress
UCS	Pa	uniaxial compressive strength
E_{ir}	Pa	intact modulus of rock
G	Pa	Shear modulus of soil
G_{max}	Pa	Maximum shear modulus of soil of soil
φ	°	Friction angle
D_R	-	Soil density
RLD	-	Ratio of pile embedded depth to outer-diameter
H_{max}	N	Maximum load applied to the head of the pile
H_{min}	N	Minimum load applied to the head of the pile
H_{lim}	N	Conventional limit load
q_{net}	Pa	Net cone resistance (test CPT)

List of Appendices

1. Introduction

The offshore wind industry is expanding rapidly throughout the world. Offshore wind farms are constructed in many parts of the world. Several projects are currently under development in France. Foundation design is an essential part of the design of the offshore wind structures. Some of the most important foundation design aspects are the marine site characterization, geotechnical design and installation methodologies. Most existing offshore wind turbines are founded on single, large diameter, driven piles, also named monopiles.
The design of monopiles serving as support for offshore wind turbines offer some specific challenges such as: avoidance of resonant frequency, respect of tight rotation tolerances (<0.5° of the structure life time) and the consideration of a great number of cyclic loading. Due to the action of wind, waves and rotation of the turbine blades, monopile foundations must withstand large lateral loads and moments. Commercial software currently available for pile design do not take into account these design constraints.
At its beginning, the offshore renewable industry relied mainly on the Oil & Gas practice for the design of structures. Standards such as the API RP 2A (American Petroleum Institut) [2] were used for foundation design. Methodologies developed in the 1950s to the early 1980s for flexible piles served as references. However, first monitored monopiles highlighted that the design pile stiffness were much lower than the measured one, leading to non-optimized structures.
Many research projects took place at the start of this new industry to try to better capture the soil-structure behaviour of rigid pile at small strain and under a large number of cyclic loading. Two main Join Industry Projects (JIP) will serve as reference in the present report, the PISA (PIle Soil Analysis) [6] international project aiming at proposing a new framework for design of monopile under static loading and the French SOLCYP (SOLicitation CYclique de Pieux) [25] project aiming at characterizing the effect of cyclic loading on piles.

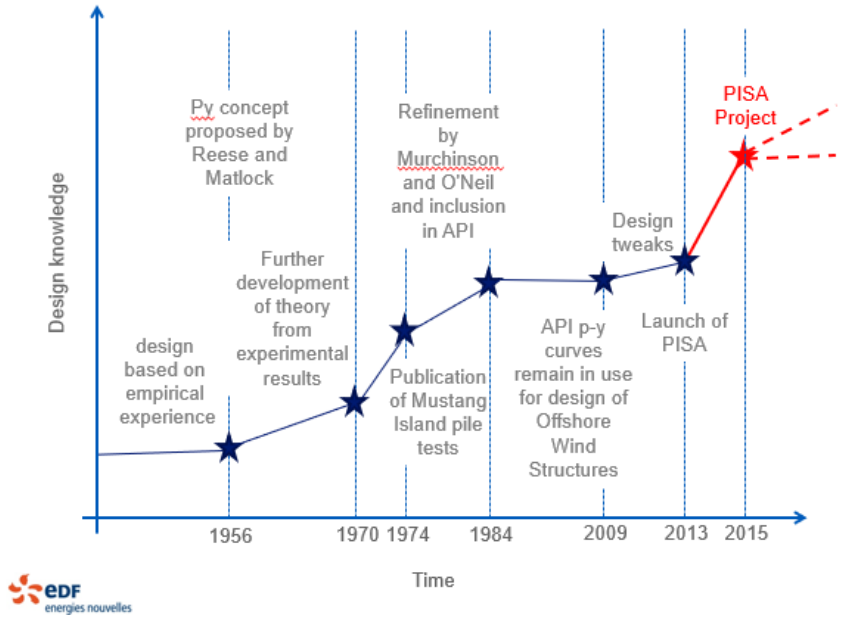

Figure 1. Design development of the laterally loaded pile

To be in a position to perform preliminary design of offshore foundations taking into consideration all above challenges, EDF EN requested to EDF R&D to build a specific design software. Having followed the main recent advancement of the industry on the topic of soil structure interaction, it was decided that the specifications of the geotechnical module would be proposed by EDF EN team.

2. Software's objectives

The objective of this internship is the description of the analysis steps in the development of a geotechnical module that computes piles subjected to lateral loading. This tool will be integrated in a special program of pre-dimensioning of offshore monopiles developed in collaboration with EDF R&D. This software will combine load calculation with structural and geotechnical analysis.
For conceptual design and verification, the input data will be :

- Environmental data : wind and wave current data
- Soil data : soil layers, ground properties, soil-structure interaction modeling method
- ULS and FLS cases description
- Wind turbine generator data : masse and inertia, tower description, material data, manufacturing data, frequency & damping wind turbine characteristics (if available), damage Equivalent Load (if available)
- Foundation data : structural data (diameter, width, length, angle), material and manufacturing data
- Calculation options & hypothesis : Wind & Wave loading options, Soil behavior options, Stresses criteria, load factors, material factors, max tower top displacement, max tower top tilt, Advanced options: for instance FLS options, FLS combination)

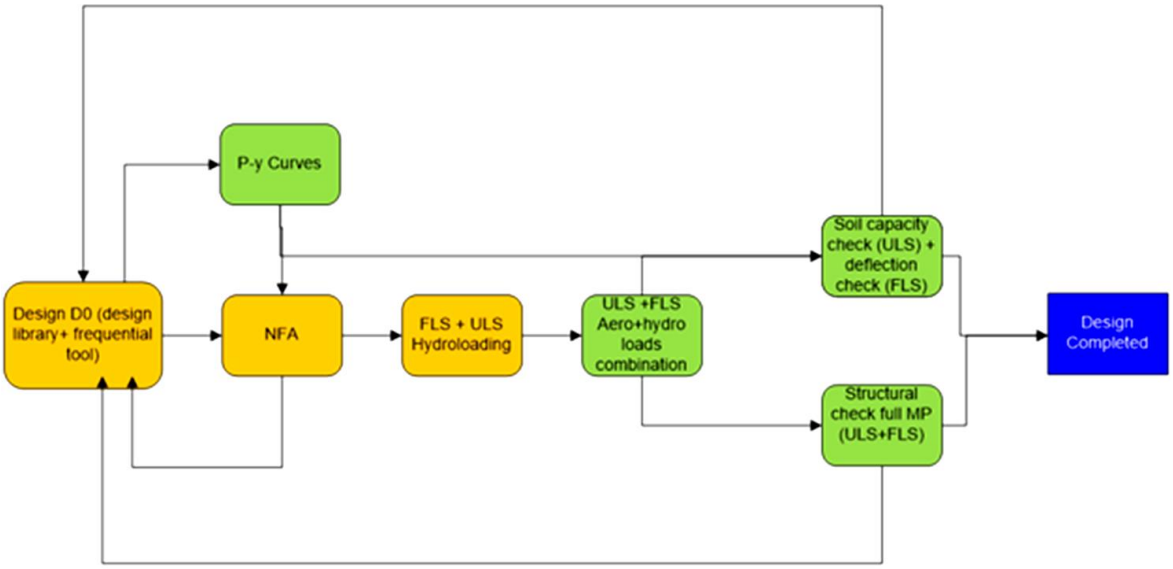

Figure 2. Design processes

The following figure visualises the principal computing modules included in conceptual design process.

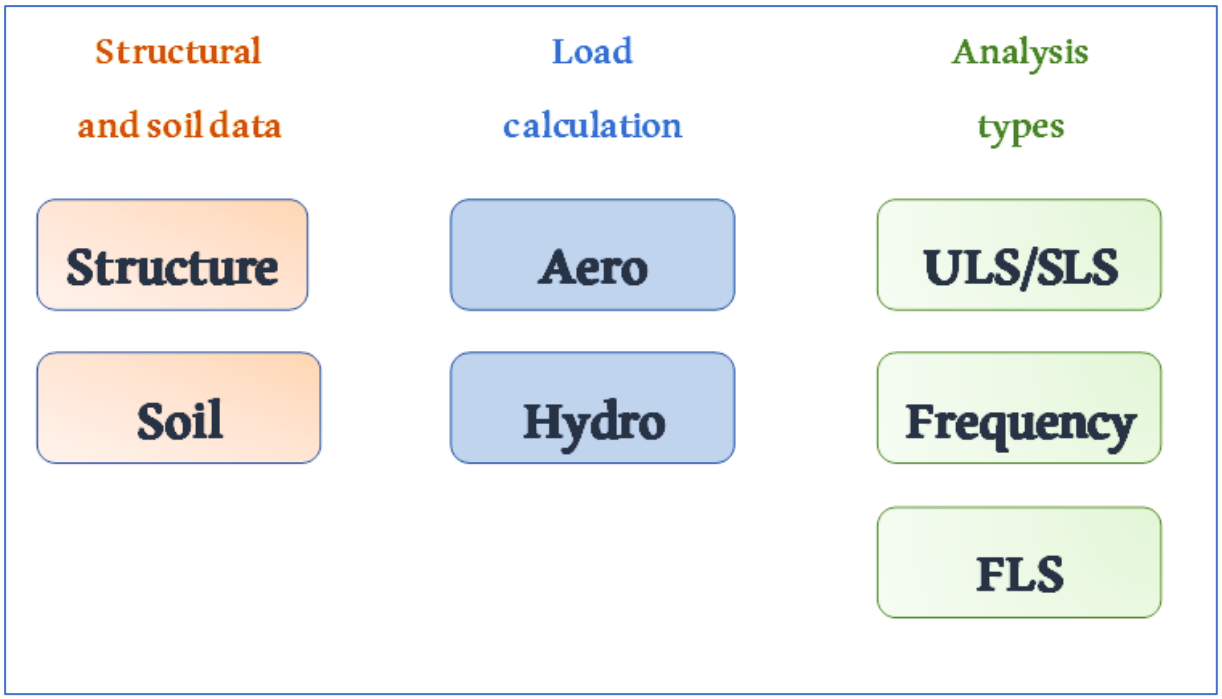

Figure 3. Principal modules included in design process

More precisely, the **structure and material** module aims at defining:

- The different objects required to perform a mechanical calculation of a structure: nodes, punctual rigidity, punctual mass & inertia, beam elements, materials, structural groups, limit conditions,
- The objects related to the final element modeling: beam finite element, punctual rigidity elements, punctual mass & inertial elements, load vectors
- The different methods associated to these objects for static and modal calculations
- The results of these calculations: displacement fields, forces & moments fields, modal shapes, modal characteristics, stresses at different positions.

Within each class of object, adequate methods will be implemented. Notably, the structural group class will contain a method for static calculation and a method for modal calculation.
This module creates and initializes all the different objects that will be used to realize a geometry and a mechanical calculation.

The goal of the **aero** module is to evaluate the aerodynamic loads on the structure to be used for static calculation. As input data, it requires an object descriptive of the environment (from the environment module), and an object descriptive of the structure. Main goal of the module is to evaluate aero loads on the tower and TP above water, expecting that the load from the rainflow analysis will come directly from the input data.

In the **hydro** module, the hydrodynamic loads will be computed. An evaluation of C_d and C_m coefficient will be possible. Hydrodynamic loadings will take into account Morison loads associated to waves and currents. An option will enable to compute the static loading associated to Archimede loads for flooded and non-flooded members.

In the **ULS/SLS** module a stress and strain computation will be achievedwith the information of other modules. A criterion on the maximum stress for ultimate load cases and on the strain for the maximum top deflection will be applied. Difference between ULS and SLS cases will be associated to the factors

applied to the loadings. The Ultimate Limit State (ULS) is the design for the safety of a structure and its users by limiting the stress that materials experience. The Serviceability Limit State (SLS) is the design to ensure a structure is comfortable and useable. This includes vibrations and deflections (movements), as well as cracking and durability.

Frequency module will enable to evaluate the modal frequency of the first mode of the structure.

FLS module intends to evaluate fatigue damage on the structure. Among the input data, wave spectrum will be provided. This module will estimate hydro and aero damping, evaluate modal characteristics using structure and material module, soil module, evaluate modal loads using hydro and aero modules and perform the damage evaluation.

Soil module will allow to compute soil reaction curves from soil data and evaluate an equivalent stiffness matrix including structure stiffness. It will be used for each type of analysis: frequential analysis, FLS, ULS, SLS. It will take into account the soil-pile system interaction in order to provide the input for structural verifications (deflection, bending moment, shear force, rotation angle). It will also perform geotechnical verifications being critical for pile predesign (critical pile length, permanent pile head rotation, soil plastification).
In terms of geotechnical predesign of offshore monopiles, as already mentioned above, available commercial software are not adapted to real offshore conditions (large diameter, excessive lateral loading, number of cycles in the range of 10^8 etc). They do not take into consideration yet recent research projects such as PISA and SOLCYP. The main objective is to incorporate within soil modeling the results of these significant recent research projects in order to improve the design methods for laterally loaded piles, specifically tailored to the offshore wind sector.

The geotechnical model will also extend the application of all the design approaches to layered soil profiles with no limit in number of layers. They will refer to the following soil types :

- Stiff naturally consolidated or slightly overconsolidated clay
- Soft preconsolidated or overconsolidated clay
- Sand (Loose, medium and dense)
- Calcareous sand
- Weak rock

Most of research efforts were focused on sand and clay soil types. However, a particularity of French soils is the common presence of carbonated weak rocks that present different behaviors and have an important impact in geotechnical design and installation methods. Therefore, for the development of the French wind industry, it is essential to understand the behavior of these rocks and include them in pre-design.

EDF EN wants to integrate all these modern methods in a modulus with functionality that will be able to generate and take into account all the special characteristics of offshore foundations.

3. Monopile design

The monopile is the most commonly used type of foundation for the installation of offshore wind turbines (Figure 4). Their design is currently based on knowledge from the oil and gas industry. However, there are major differences between the foundations of offshore oil platforms and offshore wind turbine foundations. Offshore wind turbines are designed for a life cycle of 20-25 years and the number of installed wind turbines is 20 -200 per park while in the oil industry we talk about 3 to 8 installations per platform. However, the substantial difference concerns the load to which the structure is subjected at the level of the foundation. In the case of offshore wind turbines, the predominant loads are horizontal loads and moments (high lever arm), and the ratio between horizontal load and vertical load is in the range of 70-150%. In the case of oil platforms, the vertical load is predominant and the ratio between the horizontal load and the vertical load is of the order of 10-20%.

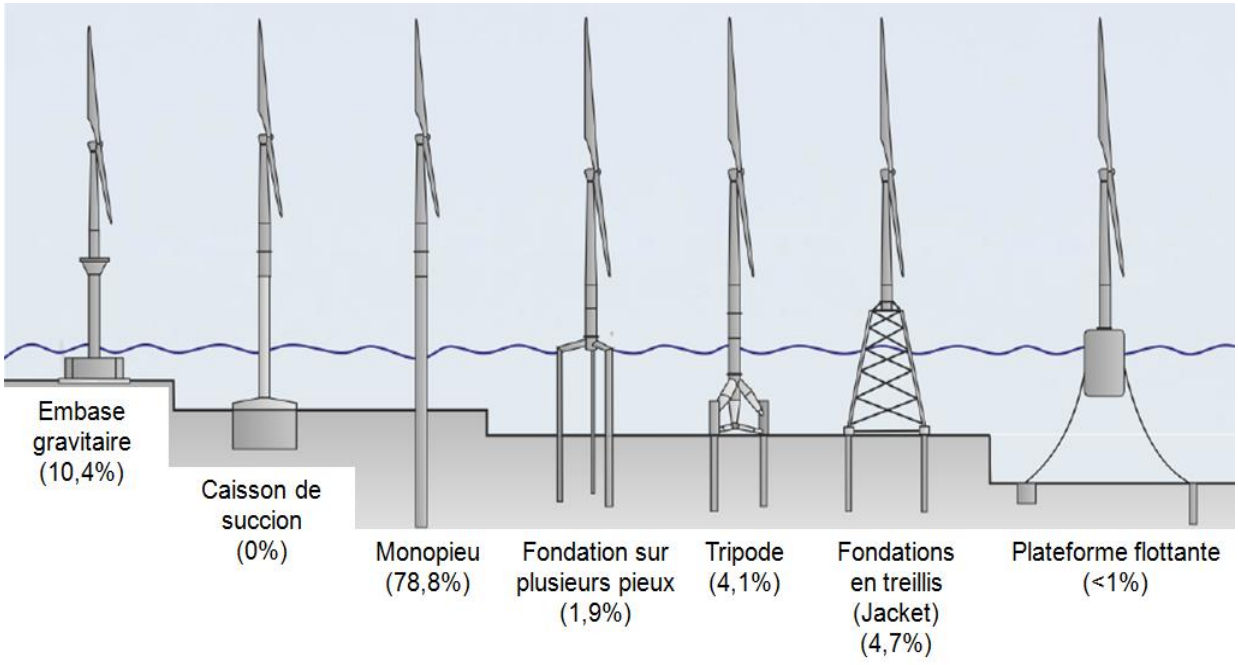

Figure 4 : Share of substructures types for wind turbines in Europe (after WindEurope and Kallehave et al. (2015)) [37]

Another particularity of monopiles is their dimensions. Ongoing European projects consider monopiles of up to 10m in diameter, with a length to diameter ratio of about 3-6. These piles tend to behave rigidly (Figure 5).However, currently used design methods are based on empirical data obtained for long, thin and flexible piles with length-to-diameter ratios greater than 10. In addition, the number of cycles to which the offshore wind structure is subjected is very important, of the order of 10^9 cycles for a 25-year life cycle.

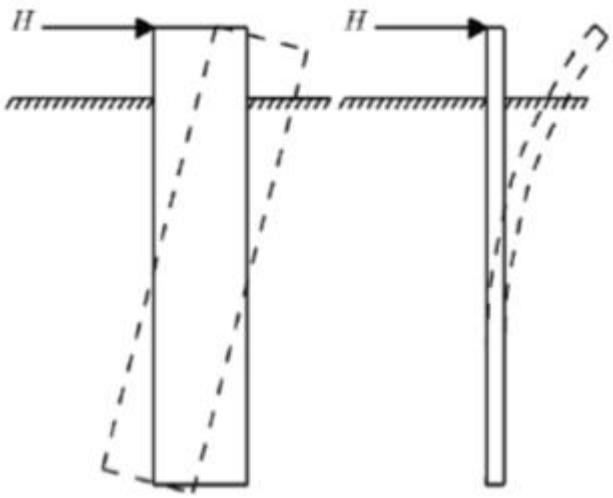

Figure 5. Rigid (left) versus flexible (right) pile behavior (after Velarde, 2016)

Monopiles are subjected to many cyclic loads with cycle frequencies spread over a large spectrum, that should avoid turbine resonant frequency. Additionally they are submitted to strict restriction with regards to maximum rotation allowable. The maximal rotation of a monopile shall not exceed 0.5 degrees at the end of its design life. These two constrains are important for monopile design, particularly since soil properties vary over time with accumulation of cycles.

The program is concentrated only on lateral analysis that is demonstrated to be more critical in the design of offshore monopiles and with great opportunities for improvement of currently used methods. Axial capacity is generally not a dimensioning aspect for monopiles, but this verification will be incorporated later in the future.

The monopile geotechnical criteria are :

- Critical pile length
- Permanent pile head rotation
- Full soil plastification

3.1 Critical pile length

The critical length L_{crit} is the length where further elongation of the pile has insignificant impact on the pile head response. It will be determined for each location for the most onerous characteristic load condition (i.e ULS unfactored loads).
The critical pile length is determined by plotting the pile head rotation as a function of the embedment length and finding the point where the change in pile head rotation relative to the minimum pile head rotation derived for an excessively long pile is at or near the flat part of the curve.
For example, we can define the critical length by allowing a maximum relative pile head rotation of 10% under characteristic ULS load, as presented in Figure 6.

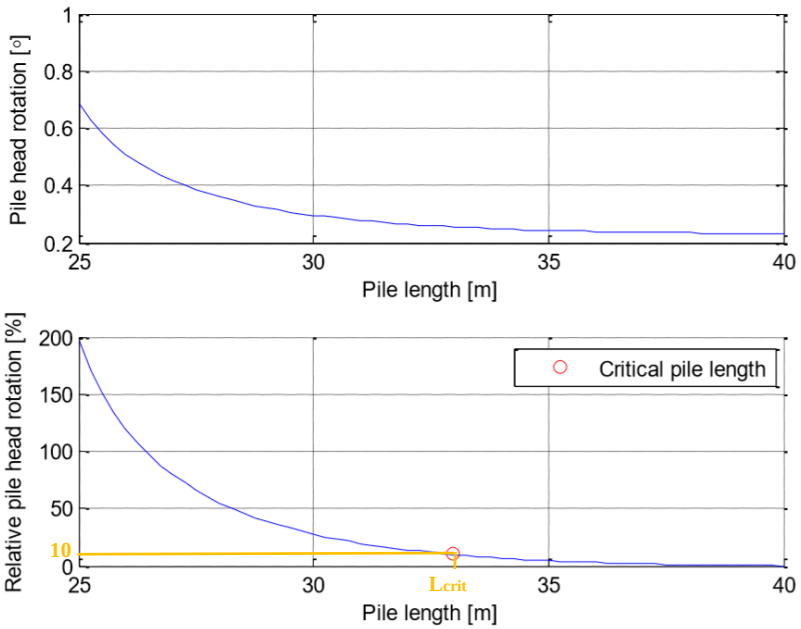

Figure 6. Example of determination of critical pile length

The determination of the critical pile length will be based on best estimate soil parameters and cyclic p-y curves for N=100 cycles (recommended value or user-defined).

3.2 Full soil plastification

A check will be also carried out to assess the utilization ratio of soil resistance along the full length of the monopile under the most onerous factored ULS load (with appropriate partial load factor applied). We compare the mobilized value of soil resistance with the calculated value of ultimate soil resistance at each p-y curve. Ultimate soil resistance is defined using best estimate soil strength parameters and applying appropriate partial factors on material strength (on S_u in case of clay, on φ in case of sand and on UCS in case of rock)

The program finally calculates the percentage of plastified soil (i.e. the ratio of length where $P > P_{ult}$ to the entire pile length).

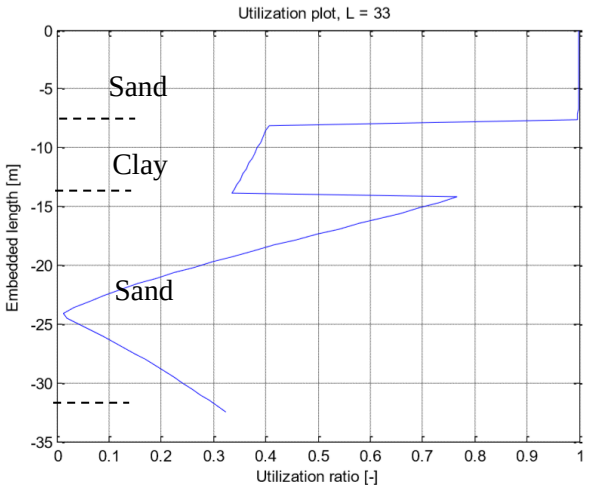

Figure 7. Utilization of p-y springs when applying design loads

3.3 Pile head rotation

Serviceability limit state (SLS) requires that permanent rotation of the pile head should be less than the maximum acceptable permanent pile head rotation which is specified by the turbine supplier.
The permanent pile head rotation is calculated as the sum of the following two contributions:

- Accumulated rotation due to characteristic ULS loading
- Accumulated rotation due to normal operation (≈30% of characteristic ULS loading considered at conceptual phase)

Figure 8 and Figure 9show the permanent pile head rotation in function with the load ratio under ULS and operational loading. The blue curve corresponds to loading part (load ratio increasing from 0 to 1) and is based on cyclic p-y curves. The red curve corresponds to unloading part (loading ratio decreasing from 1 to 0) and is based on static p-y curves. It is the pile response after unloading and is set to the initial slope of the pile response when applying p-y curves. The permanent head rotation due to characteristic or operational ULS loading is the difference between the rotation at the beginning of loading and at the end of unloading i.e. the difference between the two curves when load ratio is 0.

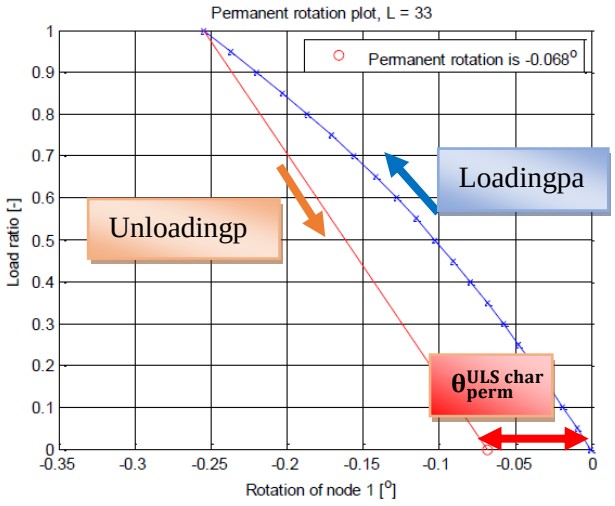

Figure 8. Estimate of permanent pile head rotation under ULS loading

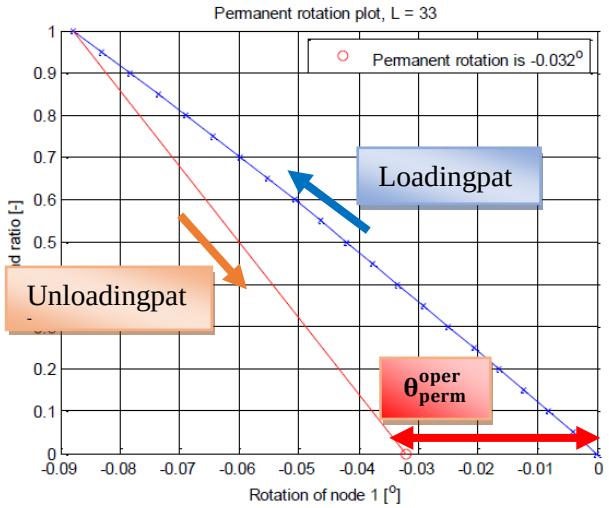

Figure 9. Estimate of permanent pile head rotation under operational loading

Total permanent pile head rotation : $\boldsymbol{\theta}^{\mathbf{tot.}}_{\mathbf{perm}} = \boldsymbol{\theta}^{\mathbf{ULSchar.}}_{\mathbf{perm}} + \boldsymbol{\theta}^{\mathbf{oper}}_{\mathbf{perm}}$

4. Methodology

4.1 Introduction

The geotechnical module will allow the user to choose between two types of soil structure approaches: Winkler or PISA [6]. Both approaches are described in the following sections.

The historical and current Winkler's (or p-y) approach (1867) is a simple method, presenting no complexity, and offers many advantages and this is why it is widely used in the offshore wind industry. However, it is based in many assumptions as it neglects identified soil-pile mechanisms which are demonstrated to be important for wind turbine monopiles. These mechanisms include vertical shear stresses on the external perimeter of the pile, a moment and a horizontal force on the base. In addition, degradation due to cyclic loading does not take into account number of cycles and magnitude of loading that is proved to play an important role on permanent deformations.
The current program will incorporate the design approach recommended by PISA project, using the classical p-y approach but extended in order to include these additional components of soil reaction.PISA offer a much more robust approach for rigid pile, it remains a static approach that does not offer yet guidance on the consideration of cyclic loading.
The following figure presents the soil reaction components that are considered in each case :

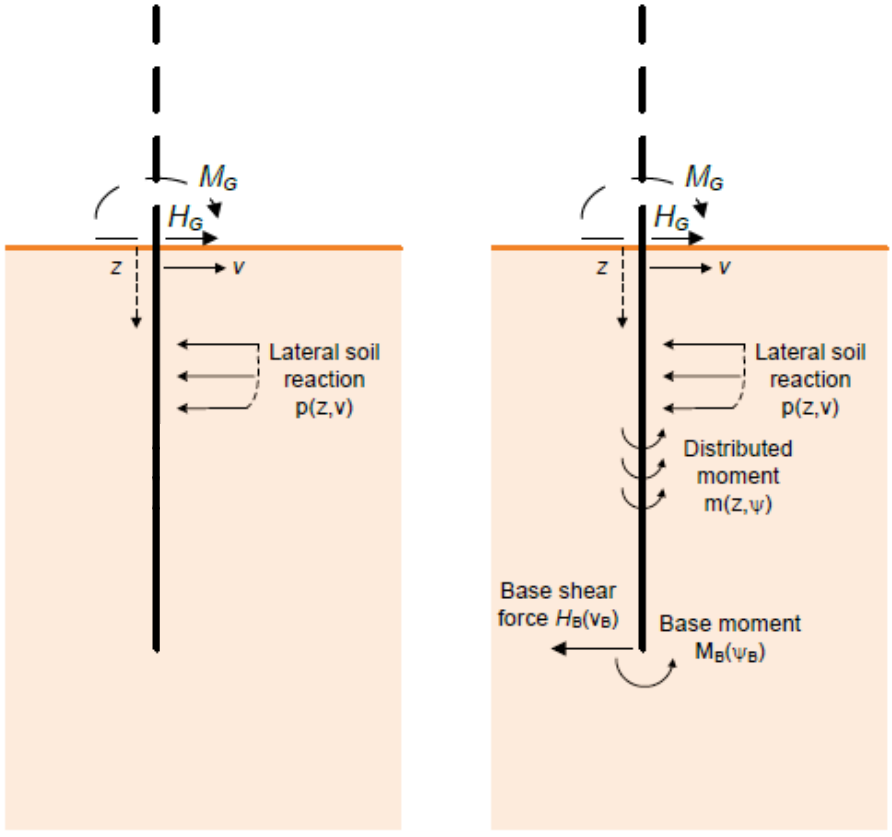

Figure 10. Components of soil reaction according to Winkler's (left) versus PISA (right) method

The application of each method to a particular design scenario is described in detail below :

4.2 Winkler's approach

The most used approach to model the lateral response of a pile is to treat the soil according to the Winkler idealization. This approach assumes that the pile acts as an elastic beam supported by a series of uncoupled horizontal elastic springs, each of which represents the local lateral soil reaction, similar to that show in Figure 11.

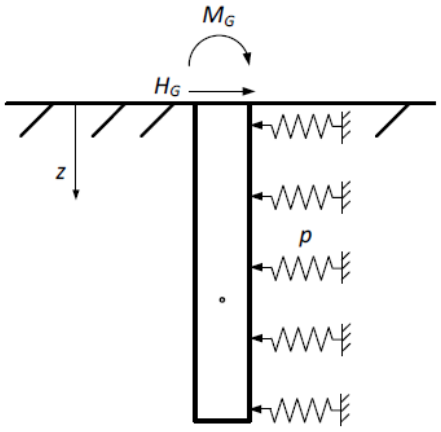

Figure 11. P-y modelling approach

These springs can be described by elastic load deflection curves (p-y curves) which take a reduction of the resistance due to stiffness and strength degradation of the sol due to cyclic loading.
The classic approach considers that there is no interaction between different loadings, i.e. the application of a horizontal load does not have any impact to the axial resistance of the pile.

The governing equation is given by

$$E_P I_P \frac{d^4 y}{dz^4} + k_{p-y} y = 0$$

- In the above equations :
- E_p = Modulus of elasticity of the pile,
- I_p = Moment of inertia of the pile,
- $k_{p\text{-}y}$ = Coefficient of horizontal soil resistance,
- y = Lateral displacement at the pile-soil boundary, and
- z = Coordinate in the axial direction of the pile.

The pressure P applied on the pile and deflection y of the soil are initially related by the following equation: $P = k_{p\text{-}y} \cdot y$. There are many different approaches available in bibliography based on laboratory tests that predict the form of the p-y curve (Matlock, Reese et al, Welch et Reese etc) for each soil type : stiff clay, soft clay, sand and weak rock and each loading condition (static and cyclic). These methods are specifically tailored to offshore monopiles.

In case of application of the current Winkler's approach, the user should select between many static and cyclic p-y approaches in order to simulate the pile-soil behaviour under different conditions. The following table presents the p-y soil models that will be available for each soil type for both static and cyclic conditions. The criterion for the choice of the P-Y methods that will be used in the soil model is the scientific method used for their definition, the loading conditions and the soil characteristics and their correspondence to the one that we find in the particular offshore site.

Table 1. Available P-y models depending on soil encountered and type of analysis

Ground behaviour		p-y data Reference Method	
		Static Loading	**Cyclic Loading**
Cohesive	**Soft soil**	• Matlock (1970) - API RP 2GEO (2000) • Modified Matlock (1970) by Stevens and Audibert (1979) • Truong & Lehane (2014) • Custom	• Matlock (1970) - API RP 2GEO (2000) • Jeanjean (2009) • Custom
	Stiff soil	• Reese & al. (1975) • Welch & Reese (1972) • Matlock (1970) - API RP 2GEO (2000) • Dunnavant (1989) • Custom	• Reese & al. (1975) • Welch & Reese (1972) • Matlock (1970) - API RP 2GEO (2000) • Modified Matlock (1979) • Dunnavant (1989) • Custom
Frictional		• O'Neil and Murchison (1983) - API RP 2GEO (2011) • O'Neil and Murchison (1983) modified by Kallehave & al. (2011) • O'Neil and Murchison (1983) modified by Sorensen & al. (2010) • Wesselink (1988) • Dyson & Randolph (2001) • Novello (1999) • Custom	• O'Neil and Murchison (1983) - API RP 2GEO (2011) • Wesselink (1988) • SOLCYP (2015) • Novello (1999) • Custom
Weak Rock		• Reese (1997) • Abbs (1983) • Custom	• Reese (1997) • Abbs (1983) • Custom

In the next section, one approach for each soil type is presented. The totality of P-y approaches available in soil module are described in detail in Appendice 1.

4.2.1 Soft clay : Matlock (1970) - API RP 2GEO (2000)

The Matlock (1970) method [20] of calculating the p-y data is presented in the API RP 2GEO (2000) [2] for soft cohesive material.
It is recommended in the case of :

- Submerged clay soils naturally consolidated or slightly overconsolidated
- Driven open-ended piles

The development of the p-y curve using Matlock (1970) consists of calculating the ultimate resistance value p_u :

$$p_u = \min \begin{cases} 3\,S_u\,D + \sigma'_v\,D + J\,S_u\,z \\ 9\,S_u D \end{cases}$$

- S_u = undrained shear strength [kPa]
- D = pile diameter at depth z [m]
- σ'_v= effective vertical stress at depth z [kPa]
- J = Dimensionless empirical constant, that has been determined by field testing[-]

We calculate the value of y_{50} as :

$$y_{50} = 2.5\,E_{50}\,D$$

- E_{50} = Strain at 50% maximum stress [-]

The parameters J and E_{50} can be selected manually. Alternatively, users can specify the clay consistency (soft, firm, stiff or hard) with the resulting parameters listed in Table 2. For soft soil, we recommend J=0.5 and E_{50}=0.02.

Table 2. Recommended Input parameters based on consistency [26]

Consistency	J	E_{50}
Soft	0.5	0.02
Firm	0.5	0.01
Stiff	0.25	0.005
Hard	0.25	0.004

The p-y curves are defined as follow

- for short term static loading :
  - $y < 8\ y_{50} : p = 0.5\ p_u \left(\frac{y}{y_{50}}\right)^{\frac{1}{3}}$
  - $y \geq 8\ y_{50} : p = p_u$

- for long term cyclic loading :

$z_r = 6\ S_u\ D / (\gamma' D + J\ S_u)$

For $z > z_r$:

- $p = \begin{cases} 0.5\ p_u \left(\frac{y}{y_{50}}\right)^{\frac{1}{3}} & \text{for } y \leq 3y_{50} \\ 0.72\ p_u & \text{for } y > 3y_{50} \end{cases}$

For $z \leq z_r$:

- $p = \begin{cases} 0.5\ p_u \left(\frac{y}{y_{50}}\right)^{\frac{1}{3}} & \text{for } y \leq 3y_{50} \\ 0.72\ p_u \left(1 - \left(1 - \frac{z}{z_r}\right)\frac{y-3y_{50}}{12y_{50}}\right) & \text{for } 3y_{50} < y < 15y_{50} \\ 0.72\ p_u \frac{z}{z_r} & \text{for } y > 15y_{50} \end{cases}$

Figure 12 presents a typical example of the p-y data for soft cohesive material using the Matlock (1970) method :

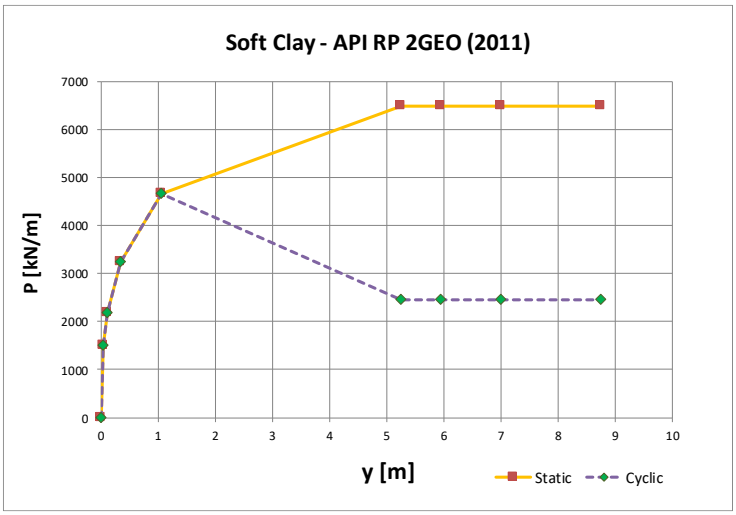

Figure 12. Typical p-y data in cohesive material following Matlock (1970)

4.2.2 Frictional soil : O'Neil and Murchison (1983) - API RP2GEO (2011)

The API RP2GEO (2011) [3] model is based on the O'Neil and Murchison (1983) [23] tangent hyperbolic method.
The ultimate resistance is calculated as

$$p_u = \min \begin{cases} (C_1\, z + C_2\, D)\sigma'_v \\ C_3\, D\, \sigma'_v \end{cases}$$

Where:
C_1, C_2 and C_3 = Coefficients depending on the soil effective angle of internal friction

- $C_1 = \frac{\tan^2\beta \tan\alpha}{\tan(\beta-\varphi)} + K_0\left(\frac{\tan\varphi\tan\beta}{\cos\alpha\tan(\beta-\varphi)} + \tan\beta\,(\tan\varphi\sin\beta - \tan\alpha)\right)$
- $C_2 = \frac{\tan\beta}{\tan(\beta-\varphi)} - K_a$
- $C_3 = K_a(\tan^8\beta - 1) + K_0\tan\varphi\tan^4\beta$

Where :

- φ = friction angle [°]
- K_0 can be defined by the user or take a value of 0.4 as recommended by API [3]
- α = φ/2,
- β = 45 + φ/2 ,
- K_a = (1 - sin φ)/(1 + sin φ) or user-defined : Rankine minimum active earth pressure coefficient

The curve is defined as:

$$p = A \cdot p_u \cdot \tanh\left(\frac{k \cdot z}{A \cdot p_u} \cdot y\right) \leq p_u$$

where

- k is the rate of increase with depth of the initial modulus of subgrade reaction [kPa/m] and can be approximated by the following equation :
  k = max(197.8 φ'^{2}-10232 φ + 136820 ; 5400 kPa) or user-defined

- $A = \max \begin{cases} 3 - 0.8\, z/D \\ 0.9 \end{cases}$ for static loading and 0.9 for cyclic loading

The development of the p-y curve of a frictional soil following O'Neil and Murchison (1983) method is presented in Figure 13.

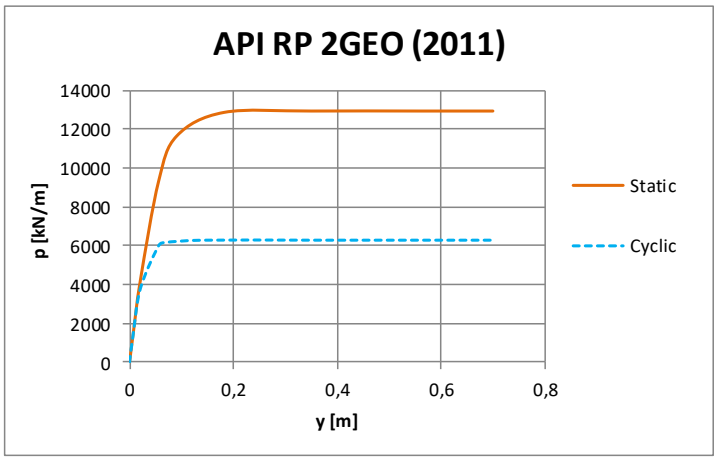

Figure 13. Typical p-y curves in frictional soil following O'Neill and Murchison (1983) method

4.2.3 Weak Rocks : Reese (1997)

The shape of the weak rock p-y curve based on Reese (1997) [27] is made up of three sections. The input parameters required for this method are,

- UCS: uniaxial compressive strength [kPa],
- α_r : the rock quality designation (percent of recovery - strength reduction factor) [-]
  or RQD= Rock Quality Designation → $\alpha_r = 1-2/3\ (RQD\%)/(100\%)$
- k_{rm} : a strain factor ranging from 0.0005 to 0.00005.
- E_{ir}: intact modulus of rock [kPa]
  It can be user-defined or calculated by the following expression : $E_{ir} = MR \cdot UCS$ where MR = modulus ratio [-]

In order to determine the exact value of k_{rm}, we have to examine the stress-strain curve of the rock sample. Typically, the k_{rm} is taken as the strain at 50% of the maximum strength of the core sample. Because limited experimental data are available for weak rock during the derivation of the p-y criteria, the k_{rm} from a particular site may be unknown. For such cases, we may use the upper bound value (0.0005) to get a larger value of y_{rm} which in turn results in the softest p-y curves and provides a more conservative result.

The development of the p-y curve for weak rock is presented in Figure 14 (static and cyclic case). The ultimate resistance for rock, p_u, is calculated from the input parameters. The linear portion of the curve with slope K_{ir} defines the curve until intersection with the curved portion.

$$p_u = \min \begin{cases} \alpha_r \cdot UCS \cdot D\left(1 + 1.4\,\frac{z_r}{D}\right) & , 0 \le z_r \le 3D \\ 5.2 \cdot \alpha_r \cdot UCS \cdot D & , z_r \ge 3D \end{cases}$$

The PY curve is defined as follow :

- $p = \min\left[\frac{p_u}{2}\left(\frac{y}{y_{rm}}\right)^{1/4}, K_{ir}y\right]$, if $y < 16y_{rm}$
- $p = p_u$ otherwise

Where

- K_{ir} is the initial stiffness, given by $K_{ir} = E_{ir} \cdot k_{ir}$
- k_{ir} is a dimensionless coefficient that is given by:
  - $k_{ir} = \begin{cases} 100 + 400 \cdot \frac{z_r}{3D} & \text{if } 0 < z_r < 3D \\ 500 \text{ otherwise} \end{cases}$
- y_{rm} is the limiting displacement for this initial elastic portion and is given by: $y_{rm} = k_{rm}D$

The general form of the p-y curve of Reese (1997) is presented in the figure bellow:

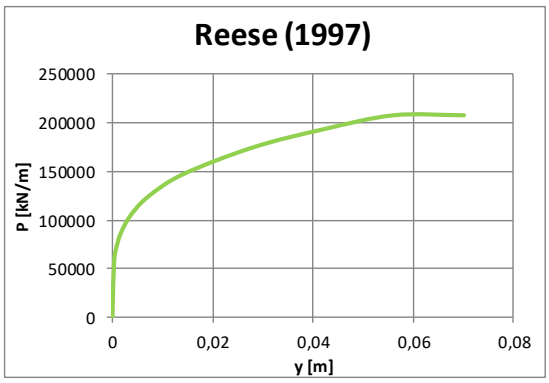

Figure 14. P-y curve for Weak Rock (Reese (1997)

4.2.4 Diameter effect on p-y curves

The widely used API recommendations adopt the soft clay criterion developed by Matlock (1970) [20] and the sand criterion originally introduced by Reese et al. (1974) [28]. The study of Reese et al. (1974) is based on 24 inch piles (≈ 0,61 m) and Matlock (1970) is based on 12.75 inch (≈ 0,30 m) piles, while the offshore monopiles have much larger diameters (5-10 m).

In Reese et al. (1974) model, the initial part of p-y curve ($p \leq p_u$) is calculated by determining a coefficient *k* that represents the rate of increase of subgrade modulus with depth. This constant is multiplied with depth z and gives the subgrade reaction modulus E_s. So, the initial part of p-y curve is independent of pile diameter D. The ultimate soil resistance is roughly proportional to diameter. The independence of pile stiffness from pile diameter can only be true in the definition of initial tangent modulus, when there is zero deflection.

The clay p-y Matlock (1970) criterion proposes a parabolic p-y curve shape with an infinite theoretical initial modulus at zero deflection and so it is independent from pile diameter, too. Pile diameter intervene in the definition of critical deflection y_{50} that defines the different parts of the curve.

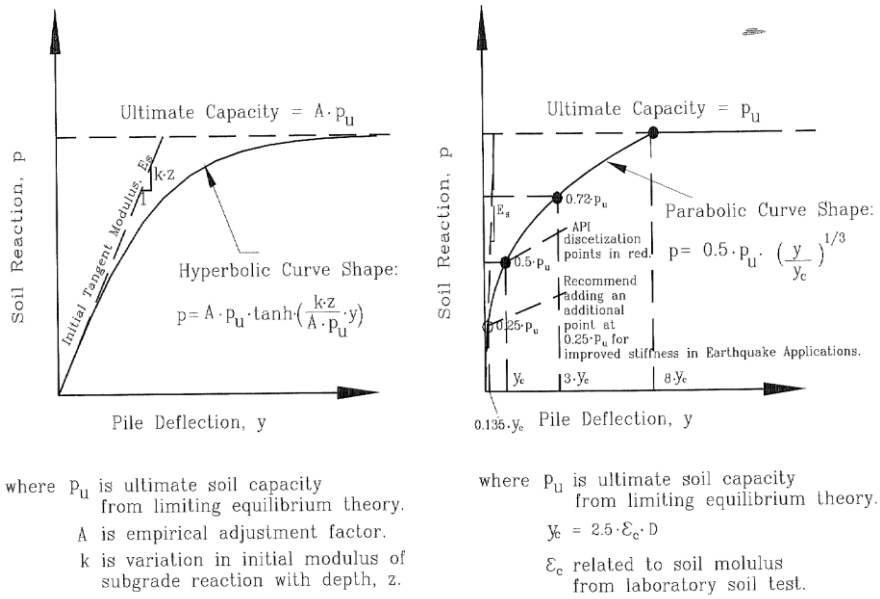

Figure 15. Review of API p-y criteria

Many studies have claimed that API RP 2A (2000) [2] may not be entirely appropriate for large diameter caissons. DNVGL-RP-C212 [5] recommended practise proposed to use the Stevens and Audibert (1979) [31] modification for monopiles with diameters between 1 and 2.5 m. Stevens and Audibert presented that, as p-y curve is influenced by pile diameters, the Matlock soft clay curve needs to be modified in order to reflect diameter effects. They compiled seven cases of full scale pile load test data in soft to medium clays, with pile diameters ranging from 11 inches (≈0,60 m) to 59 inches (≈1,5 m) and compared their results (lateral deflection, maximum bending moment) with Matlock's solution. They concluded that the currently used p-y curves lead to overestimation of the pile deflections at the groundline and underestimation of the maximum bending moment. According to them, the reason of this divergence is the assumed linear dependence between y_{50} coefficient and pile diameter. They suggested the following modification for the present Matlock (1970) method: the y_{50} coefficient used to scale the deflection array in p-y curves be changed of

$$y_{50} = 8.9 \cdot E_{50} \cdot D^{0.5}$$

Following the Stevens and Audibert paper, O'Neil and Gazioglou (1984) [24] also conducted a review on Matlock's soft clay p-y curves procedure in order to include eventual diameter effects. The proposed change is to consider a y_c coefficient that is much more complex and considerate Young modulus of pile and soil:

$$y_{50} = A \cdot E_{50} \cdot D^{0.5} \cdot \left(\frac{EI}{E_{soil}}\right)^{0.125}$$

The following table summarizes the modifications proposed for consideration of diameter effects in comparison with initial Matlock method.

Table 3. Comparison of original Matlock p-y procedures and proposed modifications

	Matlock (1970)	Stevens and Audibert (1979)	O'Neil and Gazioglou (1984)
y_{50}	$2.5 \cdot E_{50} \cdot D$	$8.9 \cdot E_{50} \cdot D^{0.5}$	$A \cdot E_{50} \cdot D^{0.5} \cdot \left(\frac{EI}{E_{soil}}\right)^{0.125}$

In the present software, we are going to incorporate the recommendation of Steven's and Audibert for large diameter monopiles, as recommended by DNV-GL practice [5].

4.3 PISA approach

PISA project [6] involves a wide range of industrial and academic partners with DONG Energy as the lead Partner and main contractor. It is conducted on two basic materials, stiff low plasticity clay and dense sand found on the Cowden clay site in the North-East of England and the Dunkirk sand site in northern France but it was extended later in other types of clay and sand densities (PISA 2 project [33]). Unfortunately it is applied only in monotonic static loading conditions, since the PISA cyclic tests are not finished yet.

PISA project focuses on the development of a new process for the design of monopile foundations for offshore wind turbine support structures. The PISA research undertook a series of field testing and three-dimensional (3D) finite element analysis aiming to develop and calibrate a new one-dimensional (1D) design model. The resulting model is based on the same assumptions and principles that underlie the Winkler's p-y method, but it is extended to provide an improved representation of the soil-pile interaction behaviour. Mathematical functions – termed 'soil reaction curves' – are employed to represent the individual soil reaction components in the 1D design model. The parameters needed to specify each soil reaction curve for a particular design scenario are determined using a set of 3D finite element calibration analyses. The soil module will incorporate the 1D design model proposed by PISA within the modelling of soil-pile interaction.

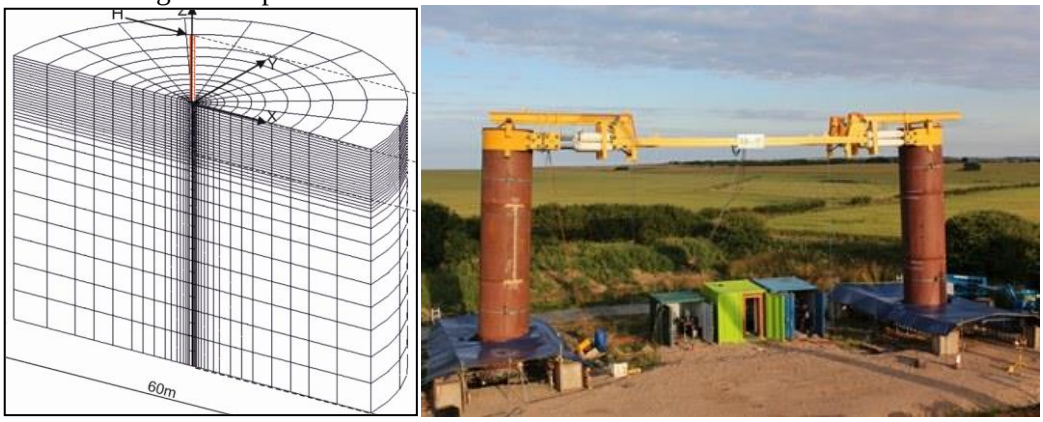

Figure 16. Example of FE mesh for the analyses of test piles (left) and photograph during tests of piles (right) [6]

According to PISA report, during 1D analysis procedure, the pile is modelled as a series of 1D beam elements according to Timoshenko beam theory. The soil/pile interaction is represented not only by a lateral distributed load applied along the pile length as in the conventional p-y approach, but also by some additional soil/pile interaction components, including a distributed moment m, a base horizontal force H_B and a base moment M_B.
Figure 17 illustrates all the components taken into account in the 1D model. In addition to the lateral distributed load p applied along the embedded pile length, a distributed moment m acting along the pile, a base horizontal force H_B and base moment M_B are included in the model.

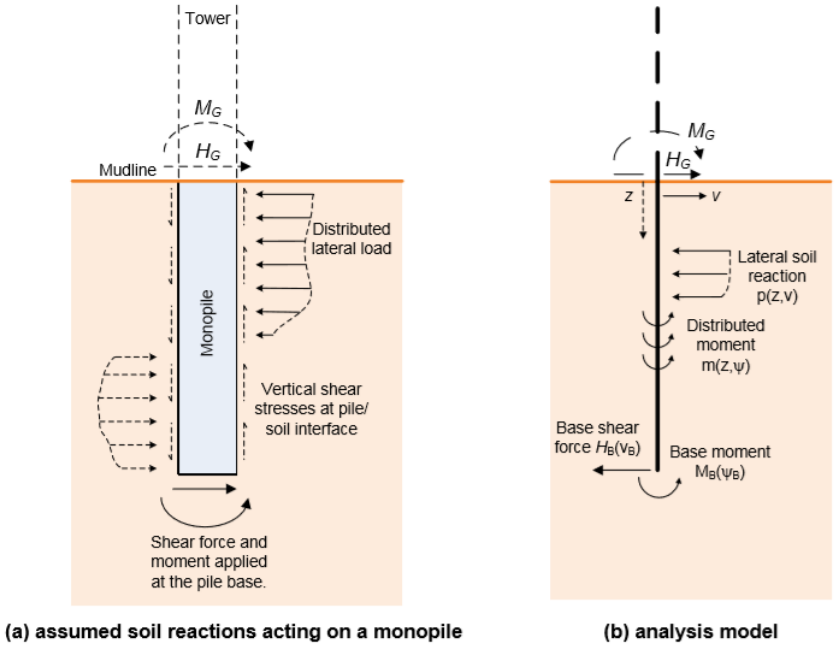

Figure 17. Component of the 1D finite element model [6]

An 1D analysis models was defined for each soil type, stiff over-consolidated clay and dense sand, based on the following procedure :

1. 3D Finite element modelling

A set of 3D finite element models was established, with varying pile geometries and loading characteristics, in order to cover a wide range of expected values. An idealized soil profile was used that resembles the ground conditions at North Sea clay and Dunkirk sand sites. The soil reaction curves are extracted.

2. Fitting of soil reaction curves

The computed soil reaction curves defined using the previous 3D finite element calibration analysis, are normalised (see Table 4), and then parameterised in order to fit to the 1D model.

3. Validation by comparison with pile tests

The 1D analysis model was validated with several pile tests. Finally, comparisons between API/DNV and 3D calibration analysis with 1D parametric model demonstrated that the accuracy of predictions of 1D model is much more important than the API/DNV approach for short and for long piles. This conclusion is also verified for arbitrary values of the geometric and loading parameters and confirms the ability of the 1D model to well predict the pile behaviour for different conditions.

More precisely, the normalisation of soil components is based on the following table :

Table 4. Normalisation of pile reaction components [6]

Component	Clay normalisation	Sand Normalisation
Distributed load, $\bar{p}$	$\frac{p}{s_u D}$	$\frac{p}{\sigma'_{vi} D}$
Lateral displacement, $\bar{v}$	$\frac{v}{D} I_R$	$\frac{v}{D} I_s \sqrt{\frac{p_a}{\sigma'_{vi}}} \left[= \frac{v}{D} \frac{G}{\sigma'_{vi}}\right]$
Distributed moment, $\bar{m}$	$\frac{m}{s_u D^2}$	$\frac{m}{pD}$
Pile rotation, $\bar{\psi}$	ψI_R	$\psi I_s \sqrt{\frac{p_a}{\sigma'_{vi}}} \left[= \psi \frac{G}{\sigma'_{vi}}\right]$
Base shear load, $\bar{H}_B$	$\frac{H_B}{s_u D^2}$	$\frac{H_B}{\sigma'_{vi} D^2}$
Base moment, $\bar{M}_B$	$\frac{M_B}{s_u D^3}$	$\frac{M_B}{\sigma'_{vi} D^3}$

The fitting procedure is then realized with the use of a conic function of the following general form :

$$-n\left(\frac{\bar{y}}{\bar{y}_u}-\frac{\bar{x}}{\bar{x}_u}\right)^2+(1-n)\left(\frac{\bar{y}}{\bar{y}_u}-\frac{\bar{x}k}{\bar{y}_u}\right)\left(\frac{\bar{y}}{\bar{y}_u}-1\right)=0$$

where $\bar{x}$ refers to a normalised displacement variable and $\bar{y}$ is the corresponding load variable.

y variables	x variables
Distributed load p	Lateral displacement v Pile rotation ψ
Distributed moment m	
Base shear load H_B	
Base moment M_B	

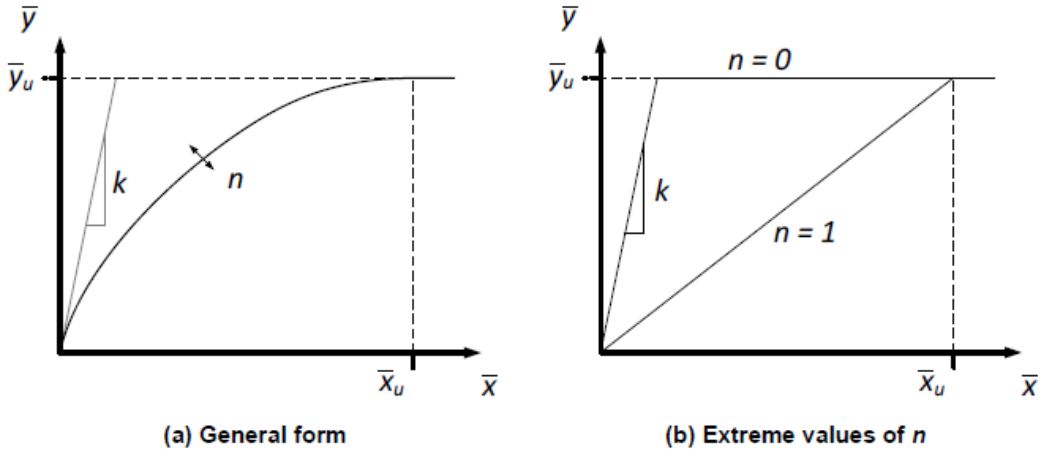

Figure 18. Function forms for soil reaction curves [6]

This function needs the definition of four specific parameters : $\bar{x_u}$, $\bar{y_u}$, k and n, where $0 \leq n \leq 1$ and $\bar{x_u} > \bar{y_u} / k$where the initial stiffness k, the ultimate response $\bar{y_u}$, the ultimate displacement $\bar{x_u}$and the

curvature n. The general form of the function is plotted in. As shown in Figure 18b, a bilinear form of the equation is obtained for a curvature parameter n = 0.

The real positive roots of $\bar{y}$ can be described by :

$$\bar{y} = \bar{y}_u \frac{2c}{-b + \sqrt{b^2 - 4ac}}; \qquad \bar{x} \leq \bar{x}_u$$

$$\bar{y} = \bar{y}_u; \qquad \bar{x} > \bar{x}_u$$

Where

$$a = 1 - 2n$$

$$b = 2n\frac{\bar{x}}{\bar{x}_u} - (1-n)\left(1 + \frac{\bar{x}k}{\bar{y}_u}\right)$$

$$c = \frac{\bar{x}k}{\bar{y}_u}(1-n) - n\frac{\bar{x}^2}{\bar{x}_u{}^2}$$

An example of the final expressions of the parameters for normalized soil reaction curves in sand for offshore conditions are presented in Table 5. The parameters are determined for piles with the following properties: 2<L/D<6, 5<D<10, 5<h/D<15, 60<D/t<110.Equations are valid for 0<z/D<6. Same table exists for the case of stiff overconsolidated clay.

Table 5. Parameters for normalised soil reaction curves in dense sand [6]

Soil reaction component	Parameter	Expression
Distributed lateral load, p	Ultimate strain, $\bar{v}_{pu}$	53.1
	Initial stiffness, k_p	$-0.85\frac{z}{D} + 7.46$
	Curvature, n_p	0.944
	Ultimate reaction, $\bar{p}_u$	$-10.18\frac{z}{L} + 21.61$
Distributed moment, m	Ultimate rotation, $\bar{\psi}_{mu}$	20
	Initial stiffness, k_m	20
	Curvature, n_m	0
	Ultimate moment, $\bar{m}_u$	$-0.05\frac{z}{L} + 0.21$
Base shear, H_B	Ultimate strain, $\bar{v}_{Hu}$	$-0.29\frac{L}{D} + 2.31$
	Initial stiffness, k_H	$-0.38\frac{L}{D} + 3.02$
	Curvature, n_H	$-0.05\frac{L}{D} + 0.94$
	Ultimate reaction, $\bar{H}_{Bu}$	$-0.07\frac{L}{D} + 0.62$
Base moment, M_B	Ultimate rotation, $\bar{\psi}_{Mu}$	50
	Initial stiffness, k_M	0.29
	Curvature, n_M	0.89
	Ultimate reaction, $\bar{M}_{Bu}$	$-0.05\frac{L}{D} + 0.38$

The PISA project had a significant contribution to the design method of laterally loaded monopiles, specifically tailored for the offshore wind sector. It has proved that currently used methods (API/DNV) underestimate the soil-pile stiffness and lead to the over-dimensioning of pile geometry. The PISA project produced a new design method that reduces the diameter, the width and the length of the pile and minimizes the installation costs. However, it was conducted on two homogeneous soil systems (Dunkirk sand and Cowden clay), while most wind farm sites are layered.

The PISA 2 [33] project carries out an additional work on layered soils in order to extend the database of soil reaction curves established during the PISA project. It applies the PISA method to different soil types and cases and it does not involve any additional laboratory or field testing. The final objective is to demonstrate the initial hypothesis that *"soil reaction curves calibrated using homogeneous soil profiles can be employed directly, to conduct 1D analyses of monopiles embedded in a layered soil"*.

Initially, the 1D model determined in PISA project is extended for some additional soil models. The 1D parametric model is finally established for the following soil types :

- London clay, representing a stiff over-consolidated plastic clay (PI~45), strongly anisotropic
- Bothkennar clay, representing a soft over-consolidated clay
- Cowden clay, represented a stiff over-consolidated low plasticity glacial clay
- Sands at three densities, (D_R = 45%, 60%, 75% and 90%)

In addition, PISA 2 extends the application of the 1D design approach to layered soil profiles. A series of layered soil models is defined, that correspond to 'problematic soil profiles' observed in real projects and site investigations. The results of 1D model were compared to the 3D finite element data. Figure 19 illustrates the layered soil configurations that were examined during analysis.

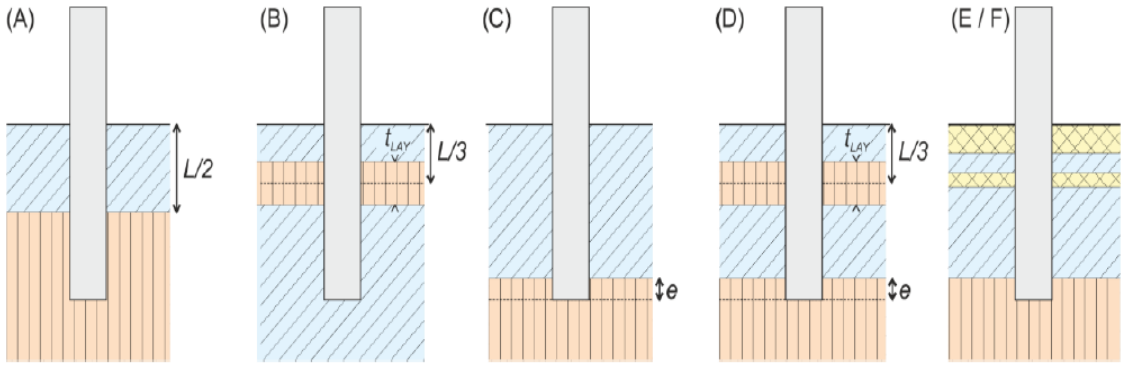

Figure 19. Layered soil configurations: (A) two layer system (B) thin layer system (C) stiff base layer system (D) conceptual multi-layer system (E/F) practical multi-layer system [33]

The investigation of a wide range of layered soil profiles and pile geometries provides a good prediction of the pile response and confirms the accuracy of the 1D parametric analysis for homogeneous as well as for layered soils. The hypothesis that *the soil reaction curves calibrated using homogeneous soil profiles can be employed to conduct 1D analysis of monopiles in a layered soil*[33], was verified at both small and larger displacements, with many 3D finite element calculations.

We can conclude that the PISA project is focused on next generation monopiles for offshore wind turbines and it proposes a method that can highly optimize offshore design and reduce construction and installation costs. On the other hand, Winkler's approach is a simple method and this is why it is

widely used in the offshore wind sector. The following table summarizes the advantages and disadvantages of each pile-soil interaction method :

Table 6. Comparison between Winkler and PISA method

Winkler	PISA
— No interaction between axial and lateral behaviour	+ Interaction between axial and lateral behaviour
+ Widely used	— Not yet incorporated in commercial software, no return of experience
+ Static & Cyclic analysis	— Static analysis only
— Flexible piles	+ Rigide piles
+ Sand, clay and rock	— Sand and clay only
	+ More precise at small displacements

5. Effects of cyclic lateral loading on p-y curves

One of the major uncertainties in the design of offshore wind turbines is the prediction of long term performance of the foundation i.e. the effect of millions of cycles of cyclic and dynamic loads on the foundation.

Classical p-y approaches do not give much attention on cyclic loading and use a simple degradation factor to reduce the ultimate soil resistance for cyclic loading. This degradation factor does not take into consideration the type of cyclic event considered and was originally developed on field tests comprising only up to 100 cycles, where only slender piles were considered.

However, monopiles are subjected to millions of small cyclic loads due to environmental forces that may change the stiffness of the combined pile-soil system and induce accumulated rotation. The behaviour of the soil-pile system under lateral cyclic loading is very complex as it should consider the impact of many different parameters like ground conditions, pile properties and load characteristics. Table 7 and Table 8 present the models that take into account some of these additional parameters and were examined during soil module's conceptual phase.

Table 7. Summary of current models for taking into account cyclic effect in sand

Model	Study method	Tests	D (m)	L/D (m)	Ground condition	Max cyclic number	Type of cyclic loading
Little & Briaud (1988)[18]	Field tests	6	0.51 ~ 1.065	32.3 ~ 60	Loose, Medium Sand	20	One way $H_{min}/H_{max} \geq 0$
Long & Vanneste (1994)[19]	Database study	34	0.145~1.43	3.1~84.1	Loose, Dense Sand	500	Two-way and one-way $-1<H_{min}/H_{max}< 0.5$
Lin & Liao (1999)[17]	Database study	20	0.145~1.43	3.1~84.1	Loose, Dense Sand	500	$-1<H_{min}/H_{max}< 0.1$
Vendure et al. (2003)[34]	Centrifuge tests	5	0.72	16.7	Dense	50	One way $H_{min}/H_{max} \geq 0$
LeBlanc et al. (2010)[15, 16]	Lab 1 g tests	15	0.08	4.5	Loose, Medium Sand	65370	Two-way and one-way $-1<H_{min}/H_{max}< 0.5$
SOLCYP Recommendations (2015)[25]	Centrifuge tests	62	0.72	16.7	Medium dense and dense Fontainebleau sand, dry or saturated	G : 75000 L : 2000	One way $H_{min}/H_{max} \geq 0$

Table 8. Summary of current models for taking into account cyclic effect in clay

Model	Study method	Tests	D (m)	L/D (m)	Ground condition	Max cyclic number	Type of cyclic loading
SOLCYP Recommendations (2015)[25]	Centrifuge tests	36	0.9 m	17.8	Saturated clay, slightly overconsolidated to simulate a soft clay that can be found in offshore conditions Non-saturated overconsolidated clay (OCR~4) to simulate a much stronger soil typical of onshore projects	G : 75000	One way $H_{min}/H_{max} \geq 0$

The cyclic loading models that are now selected and integrated within soil module in order to predict accumulation of displacement and/or change in stiffness of soil-pile system due to cyclic loading are presented below :

5.1 Lin & Liao (1999)

Lin and Liao (1999) [17] developed an expression for a degradation parameter t, to account for different model properties (soil density, load characteristics, pile installation method).
This was derived from 26 full-scale lateral load tests with varying slenderness ratios, installation method and load cycles and ratios. They deduced that the pile deflection for N cycles is given by

$$\mathbf{Y_N = Y_1 \times (1 + t \times \ln N)}$$

$$t = 0.032(L_{em}/T) \times \beta \times \xi \times \phi$$

$$T = \sqrt[5]{\frac{EI}{n_h}}$$

Where: ϕ, ξ, β represent the load characteristics, pile installation method, and soil density respectively. T reflects the pile/soil relative stiffness ration where E= modulus of elasticity, I= moment of inertia of pile and n_h= coefficient of soil reaction. According to Matlock and Reese (1962) [21], the depth at L/T = 5 is a fixed point for a laterally loaded pile and for L/T≥5 t becomes a fixed value.

Table 9. Lin and Liao (1999) test parameters

Number of tests	20
Pile diameters	0.145~1.43 m
RLD	3.1~84.1
Max cyclic number	500
Ground condition	Loose ,Dense Sand
Study method	Database study
Model equation	$Y_N = Y_1 \times (1 + t \times \ln N)$ $t = 0.032(L_{em}/T) \times \beta \times \xi \times \phi$

* RLD = Ratio of pile embedded depth to outer-diameter

Lin & Liao (1999) method is generalized for any pile length.

Additionally, Lin and Liao (1999) investigated the superposition of variable load amplitudes using an adapted version proposed by Stewart (1986). This theory indicates that a specific amount of permanent strain can be developed for various numbers of load cycles at different load . As a result, it is assumed that at some point the maximum strain will have accumulated independently of the size of the cyclic load, the number of cycles will differ instead. For a given load level N_a, we find the equivalent number of cycles N_b^* of a second load so that $\varepsilon_{Na} = \varepsilon_{Nb}$:

$$\mathbf{N_b^* = \exp\left(\frac{1}{t_b}\left(\frac{\varepsilon_{1a}}{\varepsilon_{1b}} \cdot (1 + t_a \ln N_a) - 1\right)\right)}$$

where t and ε_1 are the degradation factor and strain for the first load cycles for the respective load cases, a and b denote two different load levels.
The total amount of strain can be determined as follow :

$$\mathbf{\varepsilon_{N(a+b)} = \varepsilon_{1b}[1 + t_b \ln(N_a + N_b)]}$$

To determine the accumulated displacement, the relation between strain ε and displacement y, proposed by Kawaga and Kraft (1980), was used

$$\varepsilon = \frac{y}{2.5D}$$

where D is the diameter of the pile.

5.2 SOLCYP (2017)

5.2.1 General Information

SOLCYP (Cyclic Solicitations on Piles foundations) [25] is a French research project started in 2009 and ended in 2014. The main objective of this project is to improve the already existing knowledge of the behavior of piles subjected to cyclic stresses and to develop the procedures in order to account for these effects in design. Cyclic loading can have different effects on pile behaviour, such as degradation of shear strength, generation of excess pore pressures, 'fatigue' of soils and interfaces. These effects can lead to reduction of bearing capacity, liquefaction and/or augmentation of long-term displacements. The first manifestations of a degradation of soil's lateral resistance under cyclic loading is the augmentation of pile head displacement and diminution of pile stiffness with the number of cycles.

SOLCYP describes the process of *rainflow analysis*, that is capable of turning random events into ordered (idealized) series of cycles, as shown in Figure 20. However, it is not integrated yet in soil module. The method incorporated within soil module uses the final profile of idealized loading to calculate the accumulated pile displacement.

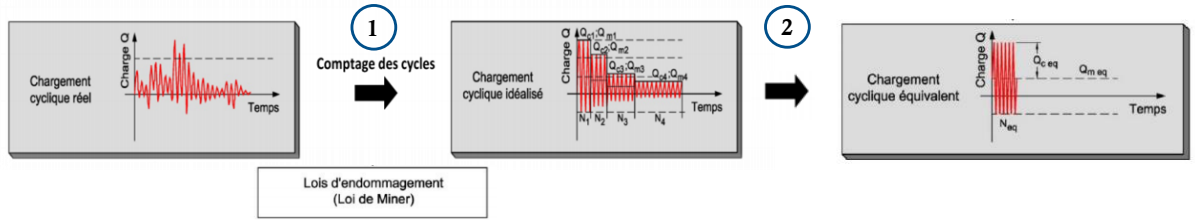

Figure 20. Rainflow analysis procedure [25]

Maximum and minimum loads applied to the pile (H_{max} and H_{min} respectively) that correspond to idealized load profile, are defined as shown in the following figure :

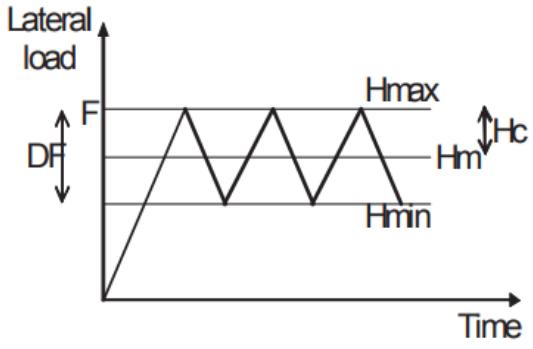

Figure 21. Load parameters required for structural geotechnical analysis [25]

The project studied both axial and lateral cyclic loading, but only results concerning lateral cyclic loading will be presented in this report. The experiments carried out for the SOLCYP project are based on two basic materials, silica sand and clays, which can be considered as reference materials.
It aims to define a method that takes into consideration the load characteristics (time histories, magnitude, number of cycles..) and predicts the cumulated rotation of the pile. All these parameters are not taken into account in the currently used API recommendations.

There are two approaches proposed by SOLCYP, the global one(SOLCYP-G), where the effect of cycles is expressed directly by increase in pile head displacement and maximum bending moment, and

the local one (SOLCYP-L), where the effect of cyclic loading is reflected in the use of cyclic p-y curves, deduced from degradation of static p-y curves.

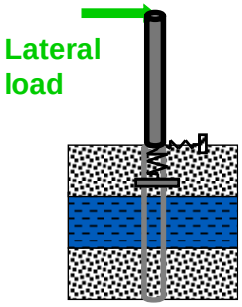

Figure 22. Global approach

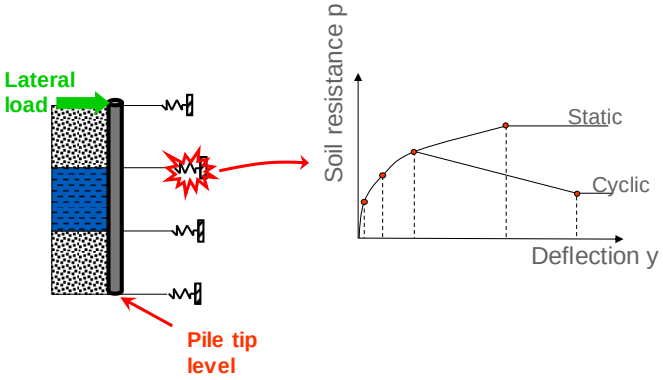

Figure 23. Local approach

The necessary input parameters for calculations are listed below:

- Pile geometry and pile stiffness E_pI_p
- Soil properties
- Characteristics of lateral cyclic loads (idealized profile)

5.2.2 Global method SOLCYP-G

This method is used to determine the pile head displacement y_N and the maximum bending moment $M_{max,N}$ after N loading cycles, based on the results y_1 and $M_{max,1}$ corresponding to 1 cycle of (static) loading. The experimental results are based on uniform soils of clay and sand.
The application of this method includes the definition of the two following parameters :

a) Conventional limit load H_{lim}, in order to ensure that the maximum load H_{max} applied to the head of the pile does not exceed the limit value.

The most commonly used methods for the determination of H_{lim} are, either the intersection of the tangent at the origin with the asymptote or the value of H corresponding to a limit displacement that is usually expressed as a percentage of the pile diameter (usually 10% D). SOLCYP adopts a combination of these two methods presented in Figure 24 : On the static loading curve linking the pile head displacement y to the load applied at pile head H, the value of limit load is given by the intersection of the vertical axis H with the line linking the two points H(y=D/2) and H(y=D).

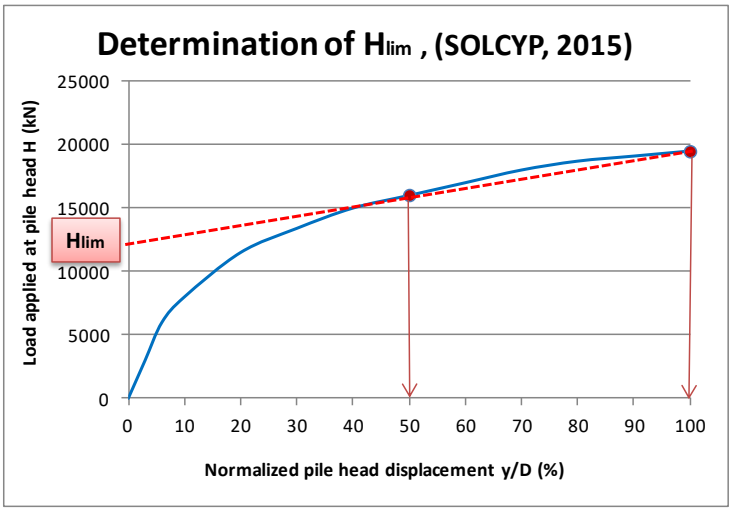

Figure 24. Example of the SOLCYP method for determination of H_{lim}

The value of limit load is therefore equal to

$$H_{lim} = 2 \cdot H(y=D/2) - H(y=D)$$

The load H(y=D) producing a pile head displacement equal to pile diameter is called failure load H_r.

b) Stiffness boundary values $(E_pI_p)_{fl}$ and $(E_pI_p)_{ri}$ that correspond to the behaviours of flexible piles and rigid piles respectively, under lateral load H_{lim}.

The relative pile head displacement y/D under a given load varies with the relative stiffness E_pI_p of the pile as shown in Figure 25. In fact, when the pile is rigid the head displacement is small and practically independent of pile stiffness, while the head displacement of a flexible pile is much bigger and dependent of pile rigidity. This is why the determination of the values of the bounds $(E_pI_p)_{fl}$ and $(E_pI_p)_{st}$ is necessary in order to take into account the relative stiffness in the global method of determining pile behaviour under cyclic loading. These values must be determined by calculations of the lateral displacement of the pile under the load H_{lim} for different values of the stiffness (E_pI_p).

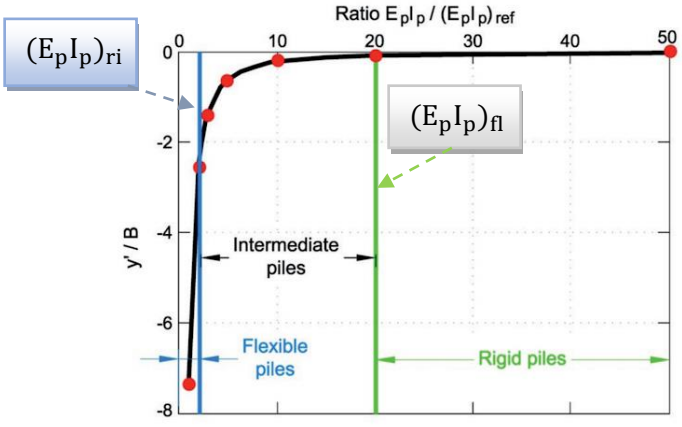

Figure 25. Example of determination of stiffness boundary values $(E_pI_p)_{fl}$ and $(E_pI_p)_{ri}$ [25]

Sand

The below equation is recommended in the case of cohesion-less soils of medium to high density (I_D greater than 50%), for which cyclic loading tends to degrade the soil response :

$$\frac{y_N}{y_1} = 1 + \frac{0.235}{CR} \cdot \log(N) \cdot \left(\frac{H_c}{H_{max}}\right)^{0.35}$$

Where

- y_N is the lateral pile head displacement after N cycles
- y_1 is the lateral pile head displacement at the same load if the loading would have been static equal to H_{max}
- H_{max} is maximum load applied to the head of the pile
- H_c is half-amplitude of the load variation
- CR is rigidity coefficient introduced in SOLCYP, which is higher than unity for rigid pile and equals to one for flexible pile:

$$CR = \left(\frac{E_p I_p}{(E_p I_p)_{fl}}\right)^{\frac{1}{5}}$$

where $E_p I_p$ is the actual pile stiffness and $(E_p I_p)_{fl}$ is the stiffness boundary for flexible piles below which the pile is considered as flexible. In this case CR=1. The following table summarizes the various expressions of the stiffness coefficient CR in function with the pile's stiffness EI.

Table 10. Values of stiffness coefficient CR in function with pile stiffness [25]

Type of pile	Stiffness $E_p I_p$ of pile	Stiffness coefficient CR
Flexible	$E_p I_p \leq (E_p I_p)_{fl}$	CR= 1
Intermediary	$(E_p I_p)_{fl} \leq E_p I_p \leq (E_p I_p)_{ri}$	$CR= \left(\frac{E_p I_p}{(E_p I_p)_{fl}}\right)^{\frac{1}{5}}$
Rigid	$E_p I_p \geq (E_p I_p)_{ri}$	$CR= \left(\frac{E_p I_p}{(E_p I_p)_{fl}}\right)^{\frac{1}{5}}$

The maximum moment $M_{max,N}$ under the influence of N cycles can be deduced from the maximum moment $M_{max,1}$ under the static loading H_{max} by the following relation :

$$\frac{M_{max,N}}{M_{max,1}} = 1 + \frac{0.094}{CR} \cdot \log(N) \cdot \left(\frac{H_c}{H_{max}}\right)^{0.35}$$

In sands, we accept that the depth of the point where the maximum moment is exerted remains at the depth observed under the static loading.

Clays

In clay, the expressions were obtained on fairly flexible piles and the available data cannot take account of influence of pile stiffness as for the sands.

The normalized pile head displacements y_N / y_1 can be correctly described by :

- Normally consolidated clays

$$\frac{y_N}{y_1} = 1.1 \cdot N^{0.5\frac{H_c}{H_{max}}}$$

- Unsaturated overconsolidated clays

$$\frac{y_N}{y_1} = 1.1 \cdot N^{0.16\frac{H_c}{H_{max}}}$$

The maximum moment $M_{max,N}$ under N cycles of cyclic loading for normally consolidated or slightly consolidated saturated clays is calculated as :

$$\frac{M_{max,N}}{M_{max,1}} = N^{0.25\frac{H_c}{H_{max}}}$$

In these soft clays, unlike what was observed with sands, the depth of the point of application of the maximum moment $z_{max,N}$ increases significantly with the number of cycles as shown in the following expression :

$$\frac{z_{max,N}}{z_{max,1}} = 1.1 \cdot N^{0.22\frac{H_c}{H_{max}}} \qquad (N>1)$$

The following table summarizes the domain of application of the global SOLCYP method:

Table 11. Domain of application of the global method SOLCYP-G for sands and clays

Parameter	Limits of application of SOLCYP-G	
	Sand	Clay
Maximum lateral load	$H_{max} \leq H_{lim}$	
Maximum pile head displacement under H_{max} static	$y_1 \leq 0.25D$	$y_1 \leq 0.3D$
Cyclic component	$H_c \leq H_{max}/2$ (one way cycles)	
Number of cycles during experiment	75000	1000
Relative stiffness of pile	No limit (Flexible / Intermediate / Rigid)	Flexible ($E_pI_p \leq (E_pI_p)_{fl}$)
Boundary conditions at pile head	Free / Fixed	Free
Nature of soil	Sandy soil, non-cohesive, dry or saturated	Cohesive clay soil (Normally consolidated or Unsaturated overconsolidated)
Soil characteristics	Increasing with depth	

5.2.3 Local method SOLCYP-L

The local method is tenting to take into account the soil-pile interaction during cyclic loading by application of appropriate reduction factors to the soil reaction p-y curves deduced from static calculations. The SOLCYP experiments showed that the degradation is much more important in the upper layers and is strongly influenced by the number of cycles and the load characteristics.
Table 12 presents the values of P-multipliers r_c that have to be applied at each depth. At this stage, a local method has been developed only for sandy soils.

Sand

Table 12. Case of sands of medium or high density – Expression of coefficients r_c (P-multipliers) to be applied to the reaction P of the static P-y curves [25]

Relative depth	z/D from 0 to 1.5	z/D from 1.5 to 3	z/D from 3 to 5	z/D > 5
Multipliers r_c	$(1-4R_1)(1+4R_2)$	$(1-2R_1)(1+2R_2)$	$(1-R_1)(1+R_2)$	1

Where $R_1 = \left[\log(N) + 3\frac{H_c}{H_{max}}\right]/20$ and $R_2 = 2.5 \cdot \left[1 - 2\frac{H_{max}}{H_{lim}}\right]/100$

All these expressions are valuable if the maximum load H_{max} applied to the head of the pile does not exceed limit load H_{lim}.

The following table summarizes the domain of application of the local SOLCYP method:

Table 13. Domain of application of the local method SOLCYP-L for sands

Parameter	Limits of application of SOLCYP-L Sand
Maximum lateral load	$H_{max} \leq H_{lim}$
Maximum pile head displacement under H_{max} static	$y_1 \leq 0.25D$
Cyclic component	$H_c \leq H_{max}/2$ (one way cycles)
Number of cycles during experiment	2000
Relative stiffness of pile	Tests on flexible piles ($E_pI_p \leq (E_pI_p)_{fl}$)
Boundary conditions at pile head	Free / Fixed
Nature of soil	Sandy soil, non-cohesive, dry or saturated
Soil characteristics	Increasing with depth

6. Effect of scour

One of the most prominent risks to the offshore foundations is scouring due to the wave and current action. If the seabed consists of sandy soil, the effect of general scour is possible to be produced. This sand is constantly moving due to waves and current. When a structure is placed offshore, the structure causes local increase of the current and wave motions. This fast flowing water stirs sand particles, picks them up and transports them away from the structure, creating a hole around the structure, which may have a significant impact on the total load on the turbine. In this case, scour protection should be applied. In case the sandy layer is relatively thin, no scour protection is applied and scour effect should be included in design.

The effect of scour is commonly modelled as illustrated in Figure 26. General scour arises from overall seabed erosion, whereas local scour is considered to affect a much smaller region, within a few diameters of a pile (a typical value is 6 times the pile diameter). The effect of local scour is a reduction of the overburden pressure that reduces linearly until the overburden reduction depth. Below the overburden reduction depth the effect of local scour vanishes [11].

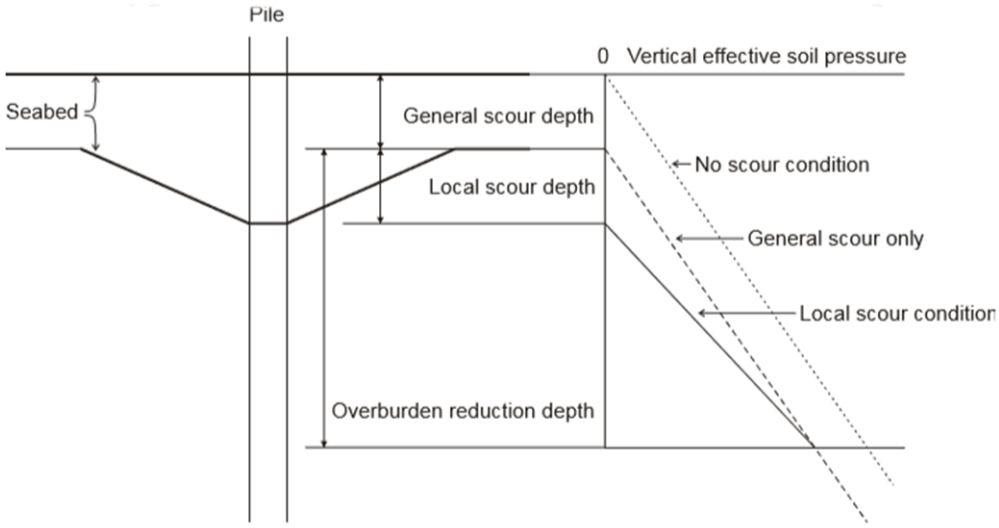

Figure 26. Overburden reduction depth determination for global and local scour

For a laterally loaded pile, the effect of scour in vertical effective stresses is leading in a modification of the ultimate lateral capacity p_u of the p-y curve.

- If neither general nor local scour is produced then the overburden pressure remains unmodified.
- If only a general scour is specified, that causes a shift to the initial profile of vertical stress so that $\sigma'_v = 0$ to the depth of scour.
- If there is specified a non-zero general and local scour, then the vertical pressure profile defined is illustrated in Figure 26deduced from the following procedure:
    - to the depth of the (general and local) scour : $\sigma'_v = 0$
    - Overburden reduction depth : it is a transition zone where σ'_v is reduced by interpolation, from 0 at the depth of scour to $\sigma'_{v,general\ scour}$ at overburden reduction depth,
    - Below overburden reduction depth : overburden pressure is only affected by general scour, $\sigma'_v = \sigma'_{v,general\ scour}$

7. Calculation process of soil module

In the following section,the different steps to follow when using the soil module will be presented (see Figure 27).

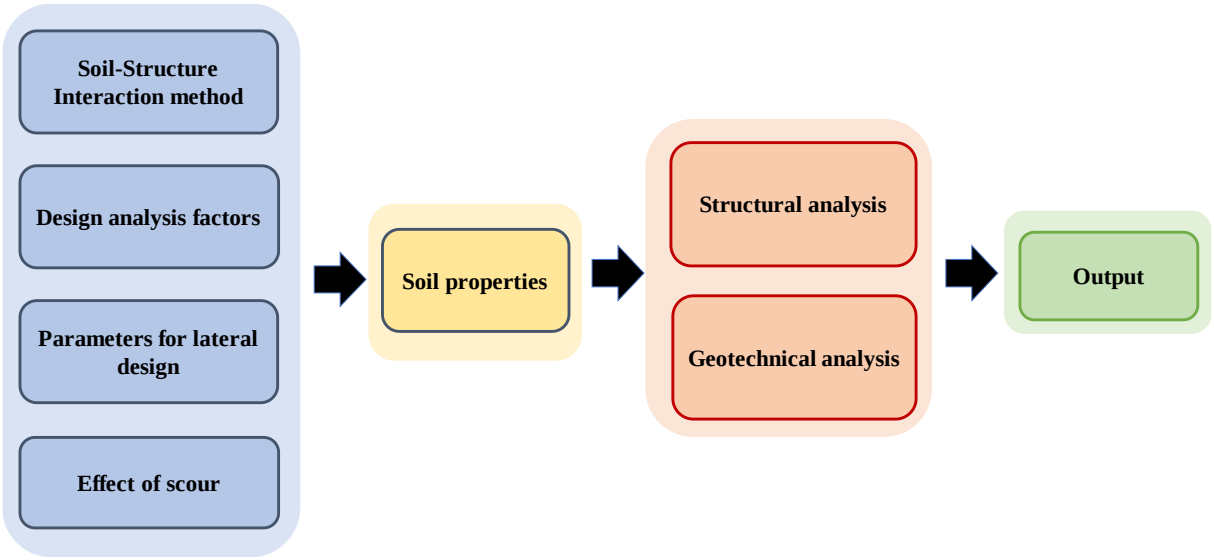

Figure 27. Soil module calculation steps

The **first step** includes the definition of input parameters required for soil modeling and for the realisation of structural and geotechnical analysis.

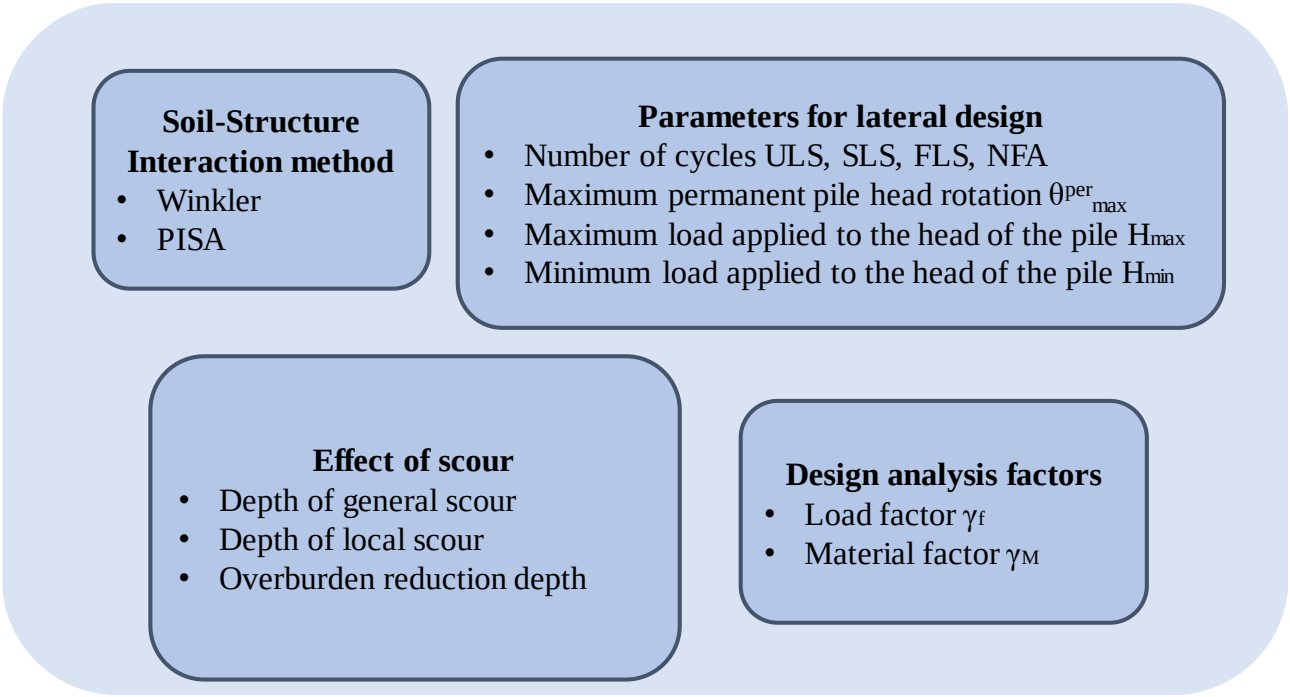

Figure 28. Input parameters for lateral analysis

It consists of :

- the selection of the appropriate soil-pile interaction method (choice between Winkler and PISA method),
- the definition of special input parameters for lateral design and more precisely :
    - The number of cycles that corresponds to each load combination (ULS, SLS, FLS, NFA) that is important in order to take into account the appropriate degradation due to cyclic loading
    - The critical value of rotation θ^{per}_{max}at pile head that refers to the second geotechnical criterion
    - H_{max} : maximum load applied to the head of the pile [kN]
    - H_{min} : minimum load applied to the head of the pile [kN]
- the consideration of scour effect (general and local scour) and
- the design analysis factors : The load and material factors γ_M and γ_f that will be used for certain analysis procedures should be specified. They are appled on particular material (soil) properties depending on soil type (on Su in case of clay, φ in case of sand and UCS in case of rock). The following table presents the recommended values by DNVGL-RP-C212 [5] for each type of analysis.

Table 14. Design analysis factors[5]

		Structural analysis	**Geotechnical design analysis**		
			Critical pile length	Permanent pile head rotation	Full soil plastification
Material factor γ_M	Sand	1.15	1.00	1.00	1.15
	Clay and Weak rock	1.25	1.00	1.00	1.25
Load factor γ_f		1.35	1.00	1.00	1.35

The **second stage** consists of modeling the ground conditions that correspond to a particular design scenario. The soil properties required depend on the soil-structure interaction method chosen in the previous step, as shown in Figure 29.

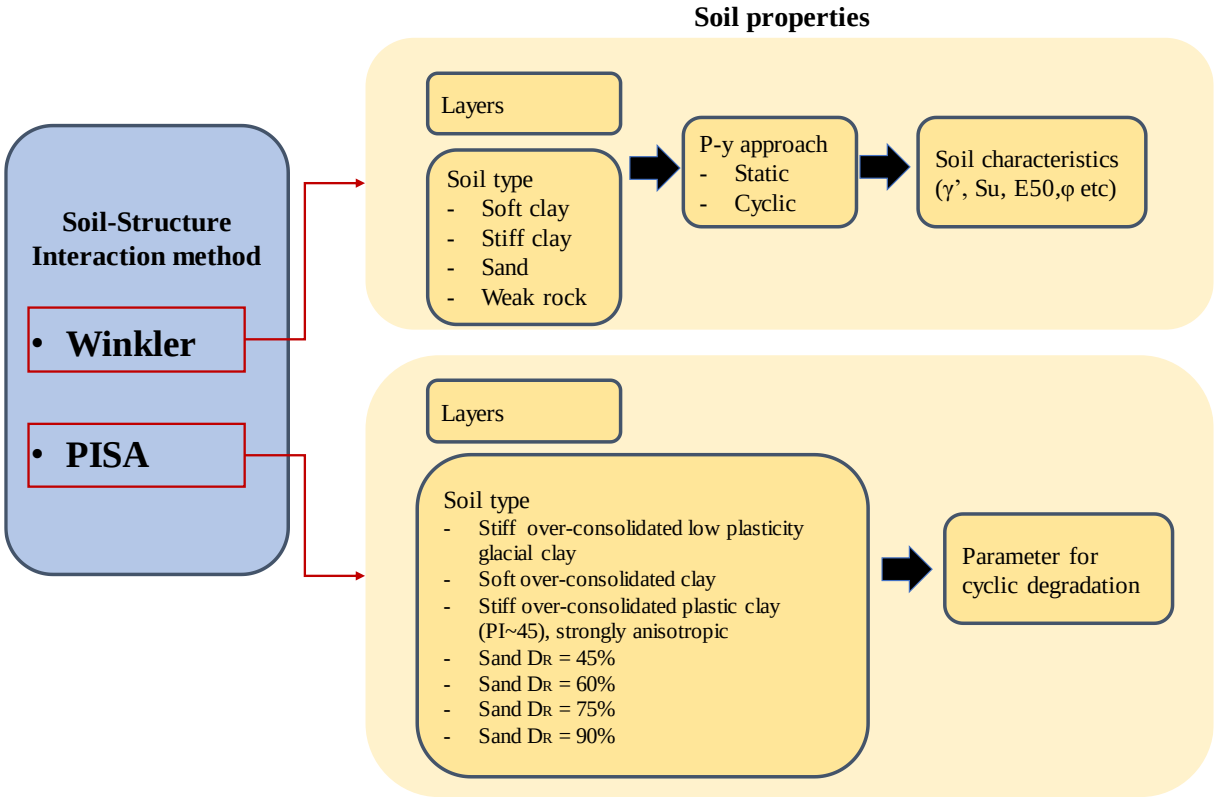

Figure 29. Definition of soil properties

Following the definition of all the necessary input parameters, the structural and geotechnical analysis are then realized. The output contains the results of structural analysis (that will be used as an input in the structure module for the realisation of structural design checks) and the results of geotechnical verifications.

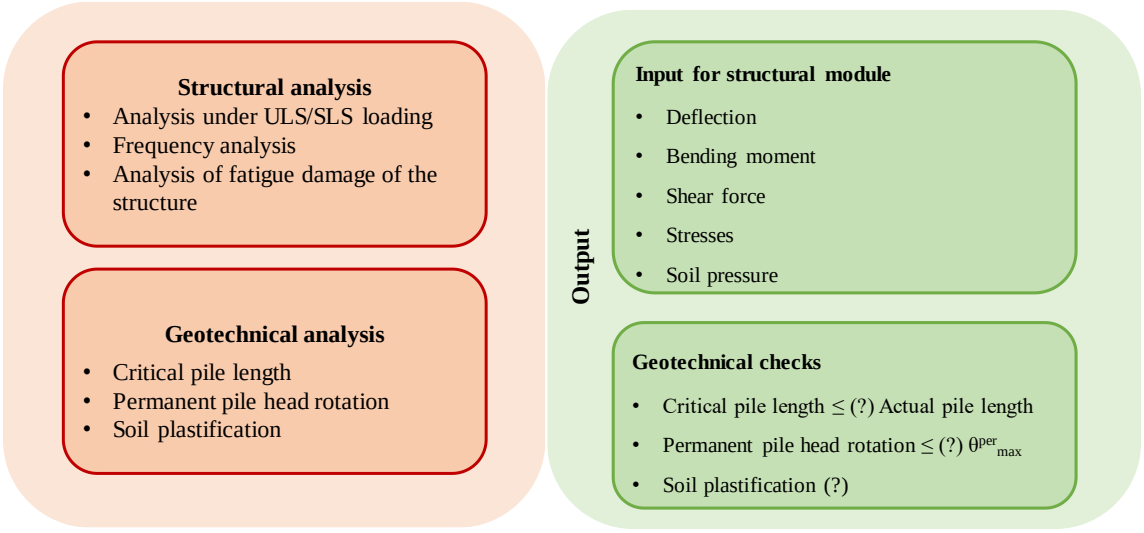

Figure 30. Analysis types and output results

The following tables summarize the types of calculation analysis required.

Table 15. Overview of geotechnical checks

Soil	Material factor γ_M	Load type	No of load cycles	Load	Linear P-y	Calculation result	GEO verification	GEO criterion
BE	1.0	cyclic	N_{ULS}	ULS	N	Pile head rotation	Critical pile length	Actual pile length ≥ Critical pile length
BE	1.0	static	N_{ULS}	ULS	Y	Permanent pile head rotation under ULS	Total permanent pile head rotation	Total rotation ≤ θ^{per}_{max}
BE	1.0	cyclic	N_{ULS}	ULS	N			
BE	1.0	static	N_{SLS}	SLS	Y	Permanent pile head rotation under SLS		
BE	1.0	cyclic	N_{SLS}	SLS	N			
BE	1.15 for frictional soils 1.25 for cohesive soils and rocks	cyclic	N_{ULS}	ULS design	N	Profile of soil pressure	Soil plastification	Mobilised soil pressure ≤ Ultimate soil resistance

Table 16. Overview of structural analysis

Soil	Material factor γ_M	Load type	No of load cycles	Load	Linear P-y	Calculation result	Structural verification	Structural criterion
BE	1.0	cyclic	N_{ULS}	ULS	N	Load-displacement curve [H-y] Deflection [y(z)] Moment [M(z)] Shear Force [T(z)] Stress [σ(z)] Soil pressure [P(z)]	(not included in soil modulus)	
BE	1.0	cyclic	N_{ULS}	ULS design	N	Load-displacement curve [H-y] Deflection [y(z)] Moment [M(z)] Shear Force [T(z)] Stress [σ(z)] Soil pressure [P(z)]		
LB	1.0	cyclic	N_{NFA}	NFA	Y	Load-displacement curve [H-y]		
BE	1.0	cyclic	N_{NFA}	NFA	Y	Load-displacement curve [H-y]		
UB	1.0	cyclic	N_{NFA}	NFA	Y	Load-displacement curve [H-y]		
BE	1.0	cyclic	N_{FLS}	FLS	N	Response [P-y]		

Some particular analysis procedures (frequential analysis, permanent pile head rotation etc), require the use of linearized soil reaction curves, that correspond to the initial slope of the linearized p-y curve. The slope of the linearized p-y curve depends on the form of the initial p-y curve and as a result of the selected p-y static approach. In certain cases the linearization of p-y curves is already considered (for example: Reese & al, 1975) while in other cases the initial slope of the p-y curve needs to be defined. In this case, we consider a very small displacement (for example 10^{-4} m) and we calculate the secant modulus of the new linear p-y curve.

8. Validation process

The final stage of this internship includes module testing and validation. It concerns the process of checking that the software code meets specifications and calculation parameters defined during conception. It also includes validating any assumption, approach prior its implementation and ensuring that it fulfills its intended objectives, in terms of optimized predesign of offshore monopiles. The validation process required the definition of a battery of test cases with a specific purpose. Three validation stages have been defined, each of which corresponding to different tests and calculation types:

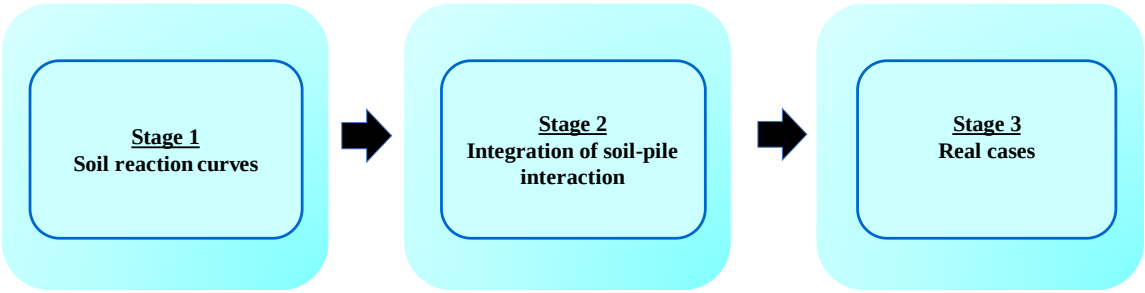

Figure 31. Validation process – Stages

The validation tools used for comparison and validation of results were OPILE, LAP and analytical approach using Excel.
OPILE is a commercial software analysing single piles subjected to axial, lateral and torsional loads, displacements and rotations [4]. OPILE allows to calculate axial pile capacity, T-Z, Q-Z and P-Y response curves, Soil Resistance to Driving and the axial and lateral pile load displacement response. It provides a valuable analysis capability for all kinds of piles, but also suits some particular requirements of the offshore geotechnical state of art (soil reaction approach for weak rocks, diameter effect by Steven's & Audibert recommendations). However, it does neglect some specific particularities that optimise lateral design analysis, including the consideration of number of cycles during cyclic loading (SOLCYP, Lin & Liao for accumulated displacements), the integration of results of PISA research project and the automatization of geotechnical verifications. It will be used during the whole process for validation of some basic results (p-y curves, deflection, bending moment, shear force, mobilized and ultimate soil pressure).

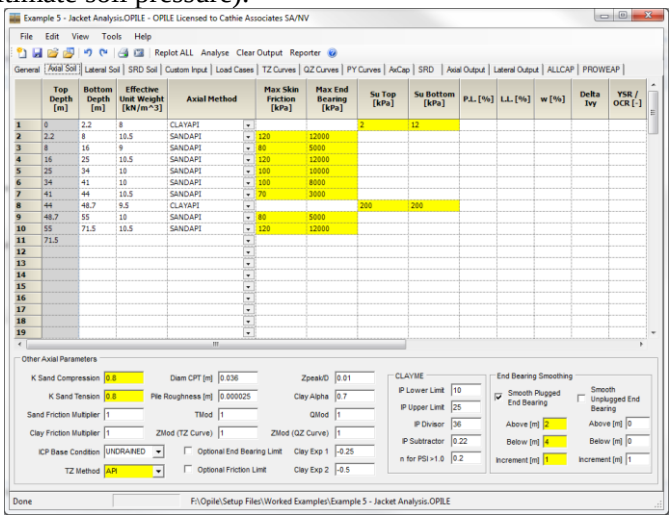

Figure 32. Definition of ground conditions in OPILE[4]

LAP (Lateral Analysis of Piles) is a simple web-based application for calculating the response of pile foundations subjected to lateral loads [12]. LAP includes both non-linear p-y models corresponding to independent (Winkler) springs, and an ability to incorporate non-linear M-theta rotational springs that are particularly important for large diameter mono-pile foundations for offshore wind turbines. The combination of non-linear horizontal and moment-rotational soil down the length of the pile can simulate the PISA approach. The program solves for the pile response using non-linear finite element analysis.

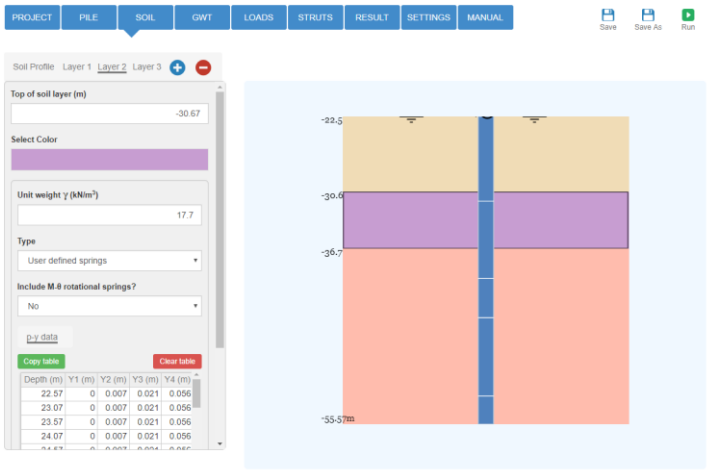

Figure 33. Definition of soil conditions in LAP[12]

The following table presents all the validation tests that where defined during validation process :

Table 17. Validation tests

Stage	Test	SSI method	Soil type	Type of loading	Soil reaction approach	Validation tool(s)
1	001	Winkler	Soft Clay	Static	Matlock (1970) - API RP2GEO (2000)	Excel OPILE
	002	Winkler	Soft Clay	Static	Modified Matlock (1970) by Stevens and Audibert (1979)	Excel OPILE
	003	Winkler	Soft Clay	Static	Truong and Lehane (2014)	Excel
	004	Winkler	Soft Clay	Cyclic	Matlock (1970) - API RP2GEO (2000)	Excel OPILE
	005	Winkler	Soft Clay	Cyclic	Jeanjean (2009)	Excel
	006	Winkler	Stiff Clay	Static	Matlock (1970) - API RP2GEO (2000)	Excel OPILE
	007	Winkler	Stiff Clay	Static	Dunnavant (1989)	Excel OPILE
	008	Winkler	Stiff Clay	Static	Reese & al. (1975)	Excel OPILE
	009	Winkler	Stiff Clay	Static	Welch & Reese (1972)	Excel
	010	Winkler	Stiff Clay	Cyclic	Matlock (1970) - API RP2GEO (2000)	Excel OPILE
	011	Winkler	Stiff Clay	Cyclic	Dunnavant (1989)	Excel OPILE
	012	Winkler	Stiff Clay	Cyclic	Modified Matlock (1979)	Excel
	013	Winkler	Stiff Clay	Cyclic	Reese & al. (1975)	Excel OPILE
	014	Winkler	Stiff Clay	Cyclic	Welch & Reese (1972)	Excel
	015	Winkler	Sand	Static	O'Neil and Murchison (1983) - API RP 2GEO (2011)	Excel OPILE
	016	Winkler	Sand	Static	O'Neil and Murchison (1983)	Excel

					modified by Kallehave & al. (2012)	OPILE
	017	Winkler	Sand	Static	O'Neil and Murchison (1983) modified by Sorensen & al. (2010)	Excel OPILE
	018	Winkler	Sand	Static	Dyson & Randolph (2001)	Excel OPILE
	019	Winkler	Sand	Static	Novello (1999)	Excel OPILE
	020	Winkler	Sand	Static	Wesselink (1988)	Excel OPILE
	021	Winkler	Sand	Cyclic	O'Neil and Murchison (1983) - API RP 2GEO (2011)	Excel OPILE
	022	Winkler	Sand	Cyclic	Novello (1999)	Excel OPILE
	023	Winkler	Sand	Cyclic	Wesselink (1988)	Excel OPILE
	024	Winkler	Sand	Cyclic	SOLCYP (2015)	Excel
	025	Winkler	Weak rock	Static	Abbs (1983)	Excel OPILE
	026	Winkler	Weak rock	Static	Reese (1997)	Excel OPILE
	027	PISA	Bothkennar Clay	Static	PISA 2 (2018)	Excel LAP
	028	PISA	Cowden Clay	Static	PISA 2 (2018)	Excel LAP
	029	PISA	London Clay	Static	PISA 2 (2018)	Excel LAP
	030	PISA	Dunkirk Sand 45%	Static	PISA 2 (2018)	Excel LAP
	031	PISA	Dunkirk Sand 60%	Static	PISA 2 (2018)	Excel LAP
	032	PISA	Dunkirk Sand 75%	Static	PISA 2 (2018)	Excel LAP
	033	PISA	Dunkirk Sand 90%	Static	PISA 2 (2018)	Excel LAP
2	034	Winkler	Soft clay	Static	Matlock (1970) - API RP2GEO (2000)	OPILE
	035	Winkler	Sand	Cyclic	O'Neil and Murchison (1983) - API RP 2GEO (2011)	OPILE
	036	Winkler	Sand Soft clay	Static	O'Neil and Murchison (1983) - API RP 2GEO (2011)	OPILE
	037	Winkler	Sand Soft clay	Cyclic	Dunnavant (1989) Reese (1997)	OPILE
	038	Winkler	Sand Stiff clay Weak rock	Static	O'Neil and Murchison (1983) modified by Sorensen & al. (2010) Reese & al. (1975) Abbs (1983)	OPILE
	039	PISA	Bothkennar Clay Dunkirk Sand 60%	Static	PISA 2 (2018) PISA 2 (2018)	LAP
	040	PISA	Cowden Clay Dunkirk Sand 90%	Static	PISA 2 (2018) PISA 2 (2018)	LAP
3	041	Winkler	Sand Soft Clay Sand	Static & Cyclic	O'Neil and Murchison (1983) - API RP 2GEO (2011) Matlock (1970) - API RP2GEO (2000) O'Neil and Murchison (1983) - API RP 2GEO (2011)	OPILE Project's design report

1. Stage 1 : Validation of soil reaction curves

The first stage aims to verify the insertion of soil reaction curves in soil module. The Winkler's p-y curves, as well as the PISA soil reaction curves, are verified at each depth in terms of ultimate soil pressure and mobilized soil reaction in function with displacement and introduced soil properties. Two validation tests are determined for each p-y approach (static and cyclic case), including comparison of p-y curves defined within soil module with the output of p-y curves in OPILE and analytical calculations using Excel (see tests 001-033,Table 17). We verify as well that the initial stiffness of the p-y curve is well defined and there are no discontinuities or aberrant results.

The following figures visualize an example of comparison results of p-y curves in soft clay following the Matlock (1970) - API RP 2GEO (2000) approach.

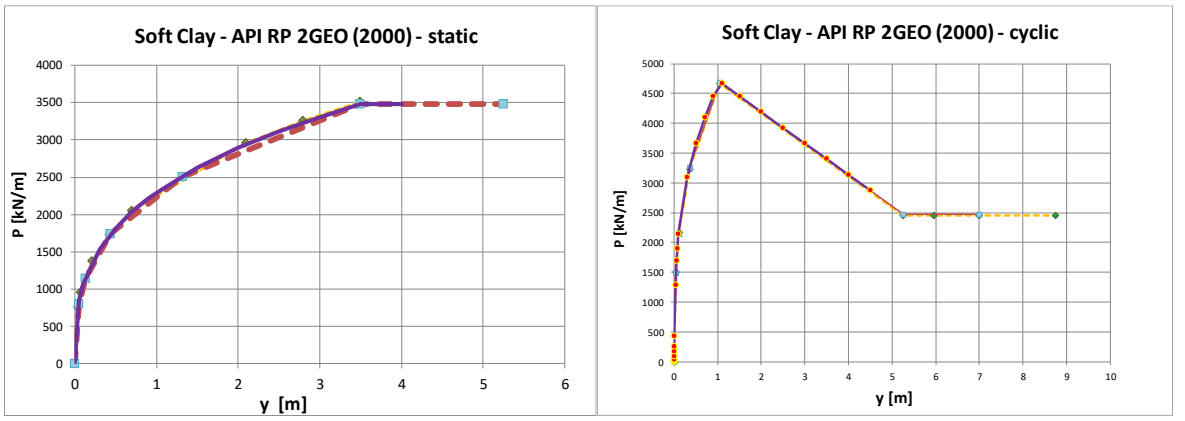

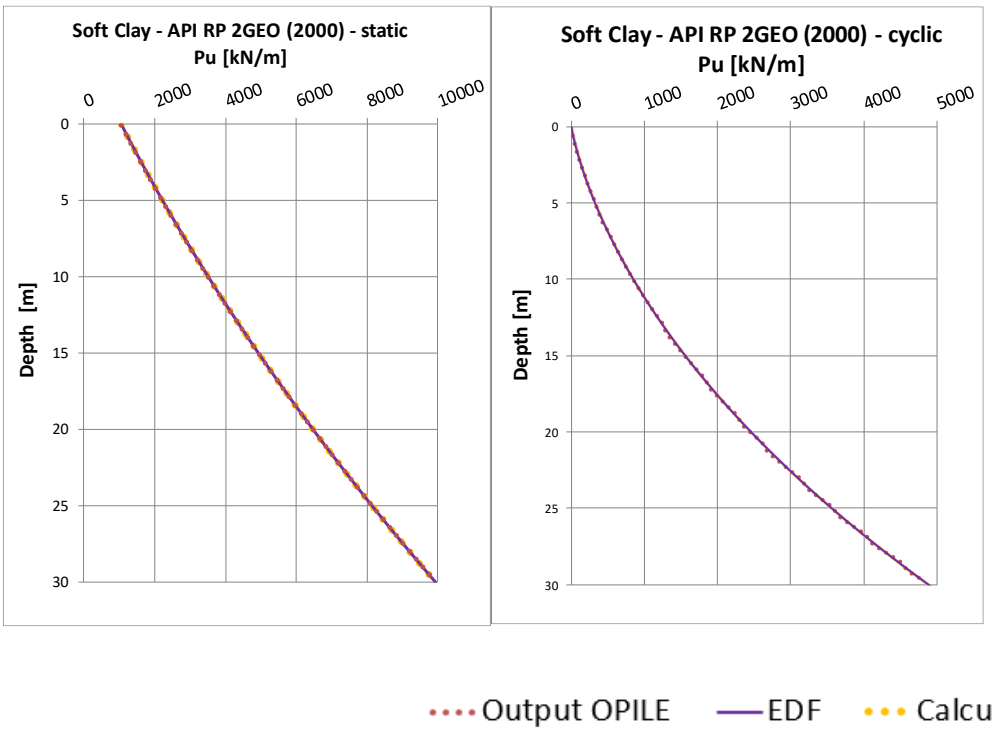

In the previous comparison curves, we introduced a comparison criterion by comparing the result given by EDF's software with those of OPILE and of analytical calculations (excel) and verifying that the error in soil pressure *p* at each displacement y does not exceed 1%:

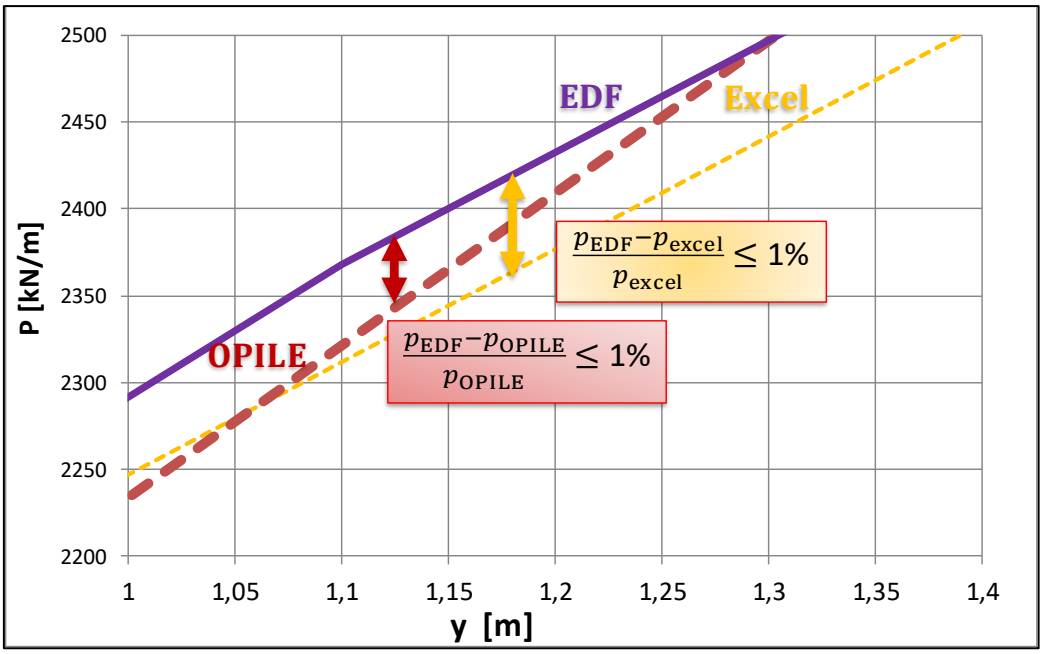

Figure 34. Comparison criterion for validation of p-y curves

2. Stage 2 : Validation of integration of soil-pile interaction instructural analysis

The objective of the second stage of validation process is to validate the consistency of the results after integration of soil reaction curves to pile-soil system modeling. The pile behavior was already validated by EDF EN in terms of displacement fields, forces & moments fields, modal shapes, modal characteristics and stresses at different positions. The validation tool used to compare and validate these results was an analytic approach (Excel-VBA). The next step is to verify that the soil reaction curves are incorporated correctly within these results and so the impact of pile-soil interaction is taken into account in an appropriate manner.

For this purpose, we created a series of validation tests (Tests 034-040 in Table 17) including various geometries, soil profiles (homogeneous and layered soil systems) and loading conditions and we compared the results of our software with OPILE output in case of use of Winkler's approach and LAP in case of use of PISA method. The results used for validation are listed below :

- Displacement y [m]
- Load-displacement curve [H-y]
- Bending moment M [kNm]
- Shear force T [kN]
- Rotation angle θ[°]
- Mobilized soil pressure P [kN/m]

The following figures visualize the comparison results of Test 38 that validate the integration of soil reaction curves within soil-pile system by implying the Winkler's p-y approach.

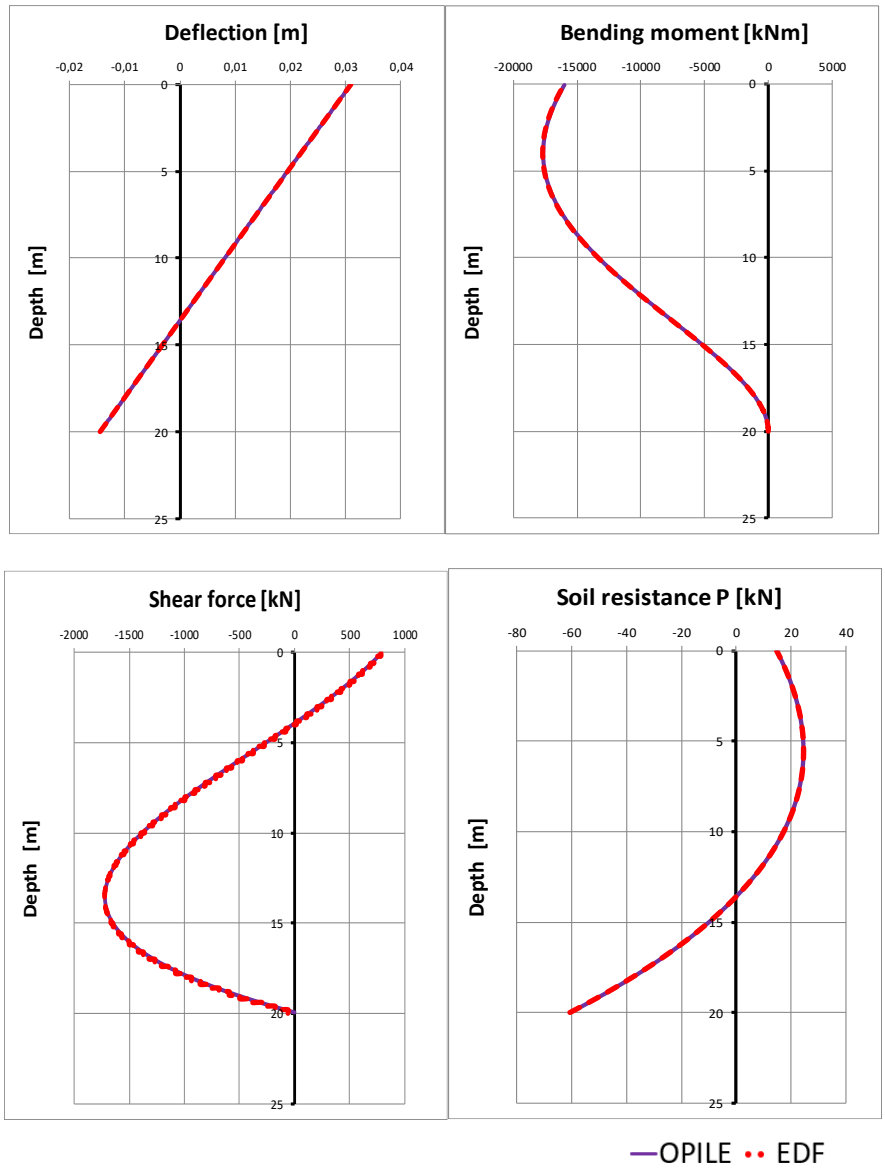

3. Stage 3 : Validation of structural and geotechnical results using real cases

The final step of validation process of soil module consists of validating the integrality of calculation analyses and results by implementing a design scenario that is part of a real offshore project (Test 041 in Table 17). The structural and geotechnical results deduced from EDF's software are compared with the results presented in the final design report of an offshore project demanding lateral analysis of offshore monopiles. The aim of this process is to demonstrate that EDF's software can provide accurate results for a particular geometry, soil and load cases that correspond to real offshore conditions and ensure that it can be used for similar cases in the future.

The comparison results that we intended to check are listed below :

- Maximum displacement
- Maximum bending moment
- Maximum shear force
- Profile of pile displacement
- Profile of bending moment

- Geotechnical verifications :
  - Critical pile length
  - Permanent pile head rotation
  - Soil plastification

The following table summarizes the results extracted from the geotechnical design report of a real offshore project and the comparison with OPILE. The table will be later completed with the results of EDF's software.

Table 18. Comparison results for a real offshore project

		Project design report	OPILE	EDF
Pile deflection at actual seabed level	mm	64	66,5	*To be completed*
Pile tip deflection	mm	-8	-8,22	
Critical pile length	m	33	33	
Permanent rotation ULS	°	0,068	-	
Permanent rotation SLS	°	0,032	-	
Total permanent rotation	°	0,1	-	
Full plastification check	-	OK	OK	

9. Conclusion

There is no doubt that EDF's software can definitely improve the design methods for laterally loaded monopiles, taking into account state of the art research projects, and it is able to incorporate in the future new, innovative solutions from the offshore wind industry.
High production and installation costs of offshore wind farms had stressed the need to overcome the shortcomings of the current methods and incorporate all the established innovative approaches in a unique software that can be used by leading industrial players for various projects all over the world. The software is particularly focused on next generation monopiles for offshore wind turbines and it incorporates methods (like PISA and SOLCYP) that apply highly innovative geotechnical engineering for design and construction and can solve important technical challenges. For example, the PISA methodology, that is an essential part of the soil module, *could deliver 30% savings on embedded steel and could save around £300,000 on each turbine foundation* according to recognized professors of engineering science. In this way, if this method is widely implemented, more offshore wind projects would be developed and renewable energy could get cheaper from fossil sources.
However, further development of the existing methods needs to be applied and then implemented in the software. PISA project is already extended, focusing now on cyclic loading, which is an essential element of safe design of offshore piles, especially for deeper water and larger turbines. The research activities aim to deliver new design methods to address this cyclic loading, through a number of research projects, including on theoretical development, soil laboratory testing and medium scale field tests. This method will be integrated in soil module and will make it possible to apply the global PISA approach in projects.
In addition, the French SOLCYP project is currently being extended in SOLCYP +. SOLCYP + is a research project in the continuity of SOLCYP that has been launched on February 2017 for a period of three years. The aim of this project is to consolidate the collaborative work between academics and industrials implied in SOLCYP on the design of offshore foundations. The project is organized around four work packages and will concern two types of soil (sand and carbonate rocks). The choice of the type of soils studied is related to the French offshore wind projects.

The implementation of all the innovative solutions in EDF software will highly optimize global design and help to create a new generation of offshore wind farms with more secure and cost-effective foundations.

10. Bibliography

1. ABBS, A.F. & NEEDHAM, A.D. (1985), Grouted Piles in Weak Carbonate Rocks, Offshore Technology Conference, Conference Paper, OTC 4852, Offshore Technology Conference.
2. API (2000), "Recommended Practice for Planning, Designing and Constructing Fixed Offshore Platforms - Working Stress Design", American Petroleum Institute Recommended Practice 2A-WSD (RP 2A-WSD), 21st edition (With Errata and Supplement 1, December 2002
3. API (2011), "Geotechnical and Foundation Design Considerations", American Petroleum Institute Recommended Practice 2A-WSD (RP 2A-WSD), 1st Edition, April 1, 2011
4. Cathie Associates SA/NV,OPILE Integrated solutions for single pile analysis, Instruction Manual, 2015
5. DNVGL-RP-C212 Offshore soil mechanics and geotechnical engineering, Edition August 2017
6. DONG Energy, University of Oxford, Imperial College London, University College Dublin (October 2016). "PISA Final Report"
7. DUNNAVANT, T.W. & O'NEILL, M.W. (1989), Experimental P-Y Model for Submerged Stiff Clay, ASCE, Journal Paper, pp. 95-114, Edition No 1, Vol. 115, Journal of Geotechnical Engineering, Editors.
8. DYSON, G.J. & RANDOLPH, M.F. (1997), Load transfer curves for piles in calcareous sand, 8th International Conference on the Behaviour of Offshore Structures, Delft, The Netherlands, Elsevier Science Ltd, 2, 245-258.
9. DYSON, G.J. & RANDOLPH, M.F. (2001), Monotonic Lateral Loading of Piles in Calcareous Sand, ASCE, Journal Paper, pp. 346-352, Edition No 4, Vol. 127, Journal of Geotechnical and Geoenvironmental Engineering.
10. Fugro Limited (1979), Memorandum, F.E. Toolan, July, 15th. Modified Matlock (1979) method
11. J. VAN DER TEMPEL, MSc, M.B. Zaaijer, MSc, H. Subroto (2004), "The effects of Scour on the design of Offshore Wind Turbines", MSc Delft University of Technology, The Netherlands
12. JAMES P. Doherty, Lateral Analysis of Piles User Manual, version 1.0, 2016
13. JEANJEAN, P. 2009. Re-assessment of P-Y curves from soft clays from centrifuge test and finite element modeling. Proceedings of the offshore technology conference, paper OTC 20158. Houston, TX.
14. KALLEHAVE, D. & LEBLANC, C. & LIINGAARD, M.A. (2012), Modification of the API P-Y formulation of initial stiffness of sand, Conference Paper, SUT OSIG, pp. 465-472.
15. LEBLANC, HOULSBY, and BYRNE, 2010a. C. LEBLANC, G. HOULSBY, and B. BYRNE. Response of Stiff Piles to Long-term Cyclic Lateral Load. Géotechnique 60, No. 2, 79–90, 2010a.
16. LEBLANC, HOULSBY, and BYRNE, 2010b. C. LeBlanc, G. Houlsby, and B. Byrne. Response of Stiff Piles to Long-term Cyclic Lateral Load. Géotechnique 60, No. 9, 715–721, 2010b.
17. LIN, S.S. & LIAO, J.C. 1999. Permanent strains of piles in sand due to cyclic lateral loads. Journal of Geotechnical and Geoenvironmental Engineering 125(9): 798–802.

18. LITTLE, R.L. & BRIAUD, J.L. 1988. Full Scale Cyclic Lateral Load Tests on Six Single Piles in Sands. Texas: Texas A&M University, College sattion.
19. LONG, J.H. & VANNESTE, G. 1994. Effects of cyclic lateral loads on piles in sand. Journal of Geotechnical Engineering 120(1): 225–244.
20. MATLOCK, H. (1970), "Correlations for Design of Laterally Loaded Piles in Soft Clay", Paper Number OTC 1204, Proceedings Second annual Offshore Technology Conference, Houston, Texas, U.S.A., Vol. 1, pp. 577-594. Matlock (1970) method description, used in cohesive soil models
21. MATLOCK, H., and LC. REESE (1962), "Generalized Solutions for Laterally Loaded Piles", Transactions (ASCE), 127, Part (1), pp. 1220—1247.
22. NOVELLO, E.A., (1999), From static to cyclic p-y data in calcareous sediments, Engineering for Calcareous Sediments, Proceedings of the 2nd International Conference, pp. 17-27.
23. O'NEIL, M. W. & MURCHISON J.M. 1983. An evaluation of p–y relationships in sands. Houston, TX, USA: American Petroleum Institute.
24. O'NEIL MW, GAZIOGLU SM (University of Houston, Texas). An evaluation of p–y relationships in clays. Report. American Petroleum Institute; 1984. PRAC 82-41-2.
25. PUECH A. & GARNIER J., Design of Piles Under Cyclic Loading, SOLCYP recommendations , 2017
26. RANDOLPH, M.F., Gourvenec, S., (2011). Offshore geotechnical engineering
27. REESE, L.C., (1997). Analysis of laterally loaded piles in weak rock. Journal of Geotechnical and Geoenvironmental Engineering. (pp. 1010-1017)
28. REESE, L. C., COX, W. R. & KOOP, F. D. 1974. Analysis of laterally loaded piles in sand. Proceedings of the offshore technology conference, paper OTC 2080. Houston, TX, .
29. REESE, L.C., Cox, W.R., and Koop, F.D., (1975), Field testing and analysis of laterally loaded piles in stiff clay, Offshore Technology Conference, OTC 2312, pp. 671-690.
30. SORENSEN, S.P.H. & Ibsen, L.B. & Augustesen, A.H. (2010), Effects of diameter on initial stiffness of p-y curves for large-diameter piles in sand, Numerical Methods in Geotechnical Engineering, CRC Press, pp. 907-912.
31. STEVENS, J.B. & AUDIBERT, J.M.E. (1979), Re-examination of PY curve formulations, Offshore Technology Conference, Paper OTC 3402, 397-403.
32. TRUONG P. & LEHANE B.M. 2014. Numerically derived CPT-based p-y curves for a soft clay modeled as an elastic perfectly plastic material. Proc. 3rd International Conference on Cone Penetration Testing, CPT'14. Las Vegas.
33. University of Oxford and Imperial College London, "PISA2 Final Report Version E", 2018
34. VERDURE, L., GARNIER, J. & LEVACHER, D. 2003. Lateral cyclic loading of single piles in sand. International Journal of Physical Modelling in Geotechnics 3(3): 17–28.
35. WELCH, R. C. & REESE, L. C. 1972. Laterally loaded behavior of drilled shafts. Research Report 3-5- 65-89. Center for Highway Research. University of Texas, Austin
36. WESSELINK, B.D., MURFF, J.D., RANDOLPH, M.F., NUENZ, I.L. & HYDEN, A.M. (1988), Analysis of Centrifuge Model Test Data from Laterally Loaded Piles in Calcareous Sand, Conference Paper, ISBN 90 6191 754 9, pp. 261-269, Engineering for Calcareous Sediments, Editors Jewell & Andrews.
37. windeurope.org

Appendices

Appendice 1 Winkler's P-y approaches

11.1 Soft clay

11.1.1 Matlock (1970) - API RP 2GEO (2000)

The Matlock (1970) [20] method of calculating the p-y data is presented in the API RP 2GEO (2000) [2] for soft cohesive material.
It is recommended in the case of :

- Submerged clay soils naturally consolidated or slightly overconsolidated
- Driven open-ended piles

The development of the p-y curve using Matlock (1970) consists of calculating the intimate resistance value p_u :

$$p_u = \min \begin{cases} 3\,S_u\,D + \sigma'_v\,D + J\,S_u\,z \\ 9\,S_u D \end{cases}$$

- S_u = undrained shear strength [kPa]
- D = pile diameter at depth z [m]
- σ'_v= effective vertical stress at depth z [kPa]
- J = Dimensionless empirical constant, that has been determined by field testing[-]

We calculate the value of y_{50} as :

$$y_{50} = 2.5\,E_{50}\,D$$

- E_{50} = Strain at 50% maximum stress [-]

The parameters J and E50 can be selected manually. Alternatively, users can specify the clay consistency (soft, firm, stiff or hard) with the resulting parameters listed in Table 19Table 2. For soft soil, we consider J=0.5 and E_{50}=0.02.

Table 19. Recommended Input parameters based on consistency [26]

Consistency	J	E_{50}
Soft	0.5	0.02
Firm	0.5	0.01
Stiff	0.25	0.005
Hard	0.25	0.004

The p-y curves are defined as follow

- for short term static loading :
  - $y < 8\,y_{50}$: $p = 0.5\,p_u\left(\frac{y}{y_{50}}\right)^{\frac{1}{3}}$
  - $y \geq 8\,y_{50}$: $p = p_u$
- for long term cyclic loading :

  $z_r = 6\,S_u\,D / (\gamma' D + J\,S_u)$
  - For $z > z_r$:

$$p = \begin{cases} 0.5\, p_u \left(\frac{y}{y_{50}}\right)^{\frac{1}{3}} & \text{for } y \leq 3y_{50} \\ 0.72\, p_u & \text{for } y > 3y_{50} \end{cases}$$

- For $z \leq z_r$:

$$p = \begin{cases} 0.5\, p_u \left(\frac{y}{y_{50}}\right)^{\frac{1}{3}} & \text{for } y \leq 3y_{50} \\ 0.72\, p_u \left(1 - \left(1 - \frac{z}{z_r}\right)\frac{y-3y_{50}}{12y_{50}}\right) & \text{for } 3y_{50} < y < 15y_{50} \\ 0.72\, p_u \frac{z}{z_r} & \text{for } y > 15y_{50} \end{cases}$$

Figure 35presents a typical example of the p-y data for soft cohesive material using the Matlock (1970) method :

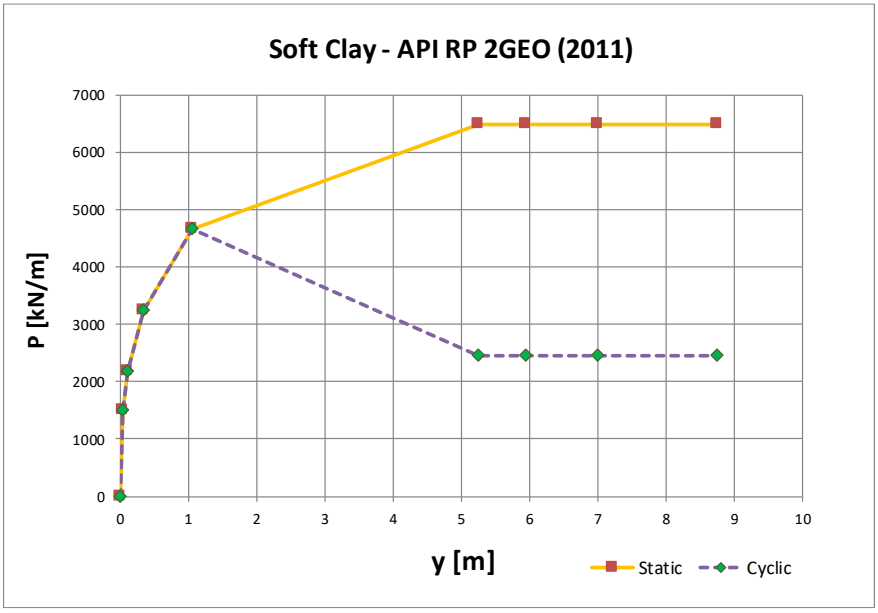

Figure 35. Typical p-y data in cohesive material following Matlock (1970)

11.1.2 Modified Matlock (1970)by Stevens and Audibert (1979)

Stevens and Audibert (1979) [31] presented that, as p-y curve is influenced by pile diameters, the Matlock soft clay curve needs to be modified in order to reflect diameter effects. They concluded that the currently used p-y curves lead to overestimation of the pile deflections at the groundline and underestimation of the maximum bending moment. According to them, the reason of this divergence is the assumed linear dependence between y_{50} coefficient and pile which underestimate the ultimate lateral soil resistance. They suggested the following modification for the present Matlock (1970) method: coefficient used to scale the deflection array in p-y curves be changed of $y_{50} = 8.9 \cdot E_{50} \cdot (D \cdot 0.0254)^{0.5}$. Steven's and Audibert modification is recommended by DNV GL standards [5]for piles with diameter between 1 and 2.5m.

11.1.3 Truong and Lehane (2014)

Truong and Lehane (2014) [32] propose this model for soft clays whose characteristics are defined by using a CPT method. They propose the following expression between the ultimate lateral resistance and net cone resistance :

Ultimate resistance : $p_u = D \cdot q_{net} \cdot \left[\left(\frac{3}{4.7+1.6 \ln I_r}\right) + (1.5 - 0.14 \ln I_r) \cdot \tanh\left(\frac{0.65z}{D}\right)\right]$

Where

- $I_r = \frac{G_{max}}{S_u}$ is the rigidity index
- z is the depth below ground surface
- D is the pile diameter

The p-y curves are then formed using the following equations :

$$p = \begin{cases} p_u \cdot \tanh\left[(0.26I_r + 3.98) \cdot \left(\frac{y}{D}\right)^{0.85} \cdot \left(\frac{z}{D}\right)^{-0.5}\right] \text{ for } \frac{z}{D} < 3 \\ p_u \cdot \tanh\left[(0.15I_r + 2.3) \cdot \left(\frac{y}{D}\right)^{0.85}\right] \text{ for } \frac{z}{D} > 3 \end{cases}$$

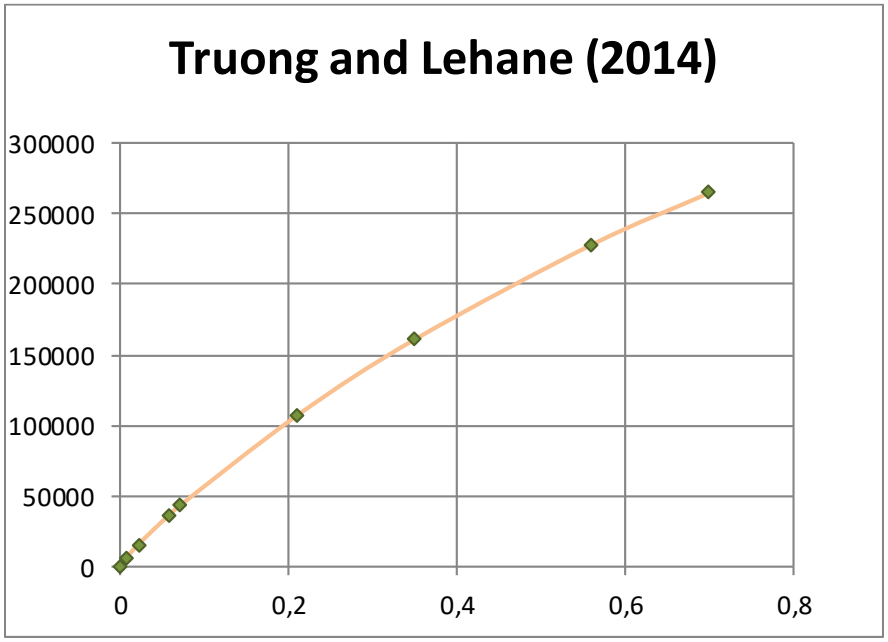

Figure 36. P-Y static curve by Truong & Lehane (2014)

11.1.4 Jeanjean (2009)

Jeanjean (2009) [13] developed p-y curves based on a series of model centrifuge tests and finite element simulations for soft clays subjected to cyclic loads. The p-y curves are given by

$$p = p_u \tanh\left[\frac{G_{max}}{100\, S_u}\left(\frac{y}{D}\right)^{0.5}\right]$$

where G_{max} is the small strain shear modulus, S_u is the undrained shear strength and D is the pile diameter. If it is not given in soil description, it can be computed according to

$$p_u = N_p\, D\, S_u$$

where

$$N_p = 12 - 4\exp(-\xi\, z/D)$$

Where

$$\xi = \begin{cases} 0.25 + 0.05\,\lambda & \text{for} \lambda < 6 \\ 0.55 & \text{for} \lambda > 6 \end{cases}$$

where

$$\lambda = \frac{Su_0}{dS_u D}$$

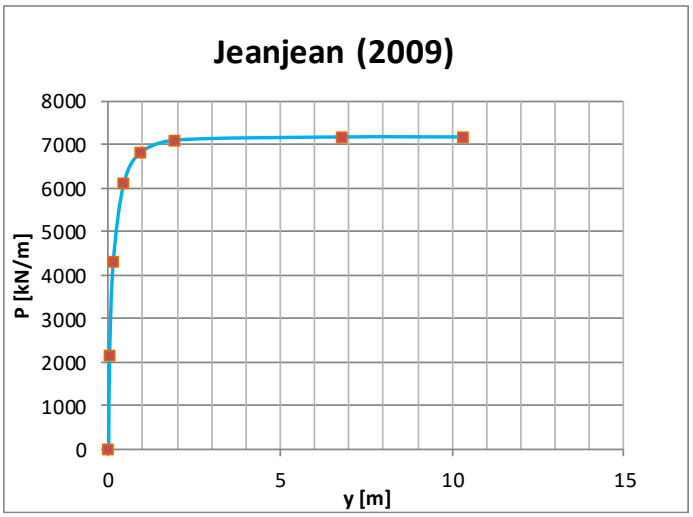

Figure 37. Typical (soft clay) Jeanjean p-y cyclic curve

11.2 Stiff clay

11.2.1 Reese & al. (1975)

The following procedure is for short-term static loading and for cyclic loading and is based on the approach of Reese & al.(1975) [29].
It is recommended in the case of :

- Stiff preconsolidated clays of marin origins, which have a secondary structure, such as fissures, joints or slickensides, with the presence of free water
- Driven open-ended piles

First, we compute the ultimate soil resistance per unit length of pile at each depth x :

$$p_u = \min \begin{cases} 2\,S_a\,D + \sigma'_v\,D + 2.83\,S_a\,z \\ 11\,S_u\,D \end{cases}$$

where

- S_a = average shear strength over the depth z : $S_a = (S_u(z=0) + S_u(z))/2$
- S_u = value of shear strength at depth z
- z = depth below seafloor
- σ'_v = effective vertical stress
- D = pile diameter at depth z

We choose the appropriate A (static and cyclic case) and B (cyclic case) for the particular depth and we establish the initial straight-line portion of the p-y curve

- For static loading :
  - for $\frac{z}{D} \leq 3$: $A = \min\left[-0.05\left(\frac{z}{D}\right)^2 + 0.29\frac{z}{D} + 0.2\,;\,0.6\right]$
  - for $\frac{z}{D} > 3$: A=0.6

  and
  - if $50 \leq S_a \leq 100$ ⇨ $k = 135 \cdot 10^3$ kN/m^3
  - if $200 \leq S_a \leq 300$ ⇨ $k = 270 \cdot 10^3$ kN/m^3
  - if $300 \leq S_a \leq 400$ ⇨ $k = 540 \cdot 10^3$ kN/m^3

- For cyclic loading :

- for $\frac{z}{D} \leq 3$: $A = \min\left[-0.05\left(\frac{z}{D}\right)^2 + 0.29\frac{z}{D} + 0.2\,;\,0.6\right]$
- for $\frac{z}{D} > 3$: A=0.6

and

- for $\frac{z}{D} \leq 1.5$: $B = \min\left[-0.055\left(\frac{z}{D}\right)^2 + 0.15\frac{z}{D} + 0.2\,;\,0.3\right]$
- for $\frac{z}{D} > 1.5$: B=0.3

and

- if $50 \leq S_a \leq 100$ ⇨ $k = 55 \cdot 10^3$ kN/m^3
- if $200 \leq S_a \leq 300$ ⇨ $k = 110 \cdot 10^3$ kN/m^3
- if $300 \leq S_a \leq 400$ ⇨ $k = 220 \cdot 10^3$ kN/m^3

We compute the critical value of displacement that corresponds to 50% of maximum strain :

$$y_{50} = E_{50} \cdot D$$

We develop the PY curve

- For static loading :
  - $y \leq A\, y_{50}$: $p = \min\left(k\, z\, y\,;\, \frac{p_u}{2}\sqrt{\frac{y}{y_{50}}}\right)$
  - $A\, y_{50} < y \leq 6\, A\, y_{50}$: $p = \frac{p_u}{2}\sqrt{\frac{y}{y_{50}}} - 0.055 p_u \left(\frac{y - A\, y_{50}}{A\, y_{50}}\right)^{1.25}$
  - $6Ay_{50} < y \leq 18Ay_{50}$: $p = \frac{p_u}{2}\sqrt{6A} - 0.411 p_u - \frac{p_u}{16\, y_{50}}(y - 6A\, y_{50})$
  - $y > 18Ay_{50}$: $p = \frac{p_u}{2}\sqrt{6A} - 0.411 p_u - 0.75\, p_u A$

  The final ultimate resistance is equal to $p_{u,f}[\text{kN/m}] = \frac{p_u}{2}\sqrt{6A} - 0.411 p_u - 0.75\, p_u A$

- For cyclic loading :
  - $y \leq 0.6\, y_p$: $p = \min\left[k\, z\, y\,;\, B\, p_u\left[1 - \left|\left(\frac{y - 0.45 y_p}{0.45 y_p}\right)\right|^{2.5}\right]\right]$
  - $0.6\, y_p < y \leq 1.8\, y_p$: $p = 0.936\, B\, p_u - 0.085\, p_u \left(\frac{y - 0.6 y_p}{y_c}\right)$
  - $y > 1.8\, y_p$: $p = 0.936\, B\, p_u - \frac{0.102}{y_c}\, p_u y_p$

  The final ultimate resistance is equal to $p_{u,f}\,[\text{kN/m}] = 0.936\, B\, p_u - \frac{0.102}{y_c}\, p_u y_p$

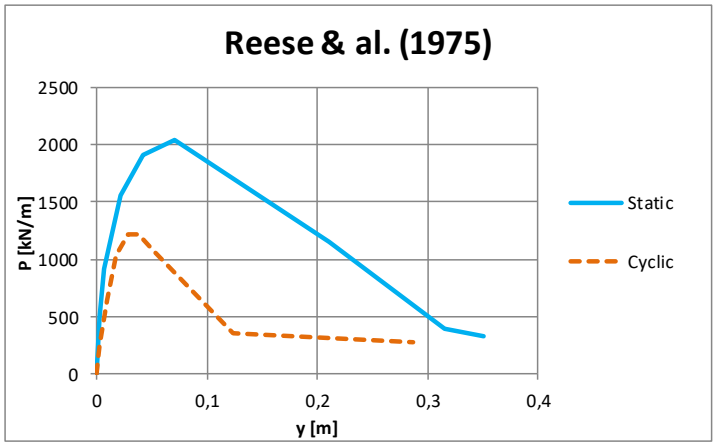

Figure 38. Static and cyclic P-y curves Reese & al.(1975)

11.2.2 Welch & Reese (1972)

According to Welch & Reese, (1972)[35], the ultimate soil resistance is calculated as follows :

$$p_u = \min \begin{cases} 3\,S_a\,D + \sigma'_v\,D + J\,S_a\,z \\ 9\,S_u D \end{cases}$$

For stiff soil, we recommend J=0.25 and E_{50}=0.005.
We select a depth and develop p-y curve using the relationship below

- For static loading :
  - $p=\frac{p_u}{2}\left(\frac{y}{y_{50}}\right)^{\frac{1}{4}}$
- For cyclic loading :

After development of the p-y curve for a static loading, we determine the number of times the design lateral load will be applied to the pile. For several values of p/p_u we obtain the value of C, the parameter describing the effect of repeated loading on deformation, from a relationship developed by laboratory tests (Welch & Reese, 1972), or in the absence of tests, from the following equations:

$$C = 9.6\left(\frac{p}{p_u}\right)^4$$

At the value of p corresponding to the values of p/p_u, compute the new values of y for cyclic loading from the following equation:

$$y_c = y_s + y_{50}\,C\,\log N$$

where

- y_c= deflection under N-cycles of load
- y_s= deflection under short-term static load
- y_{50}= deflection under short-term static load at one-half the ultimate resistance.

The p-y curve defines the soil response after N-cycles of load.

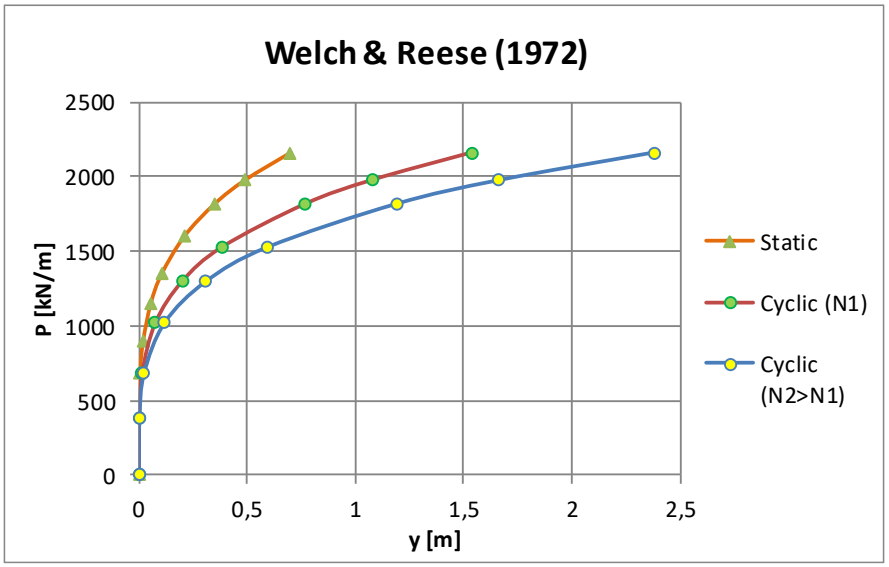

Figure 39. Static and cyclic P-Y curves (Weltch & Reese, 1972)

11.2.3 Matlock (1970)

The Matlock (1970) [20] method of calculating the p-y data is presented in the API RP 2GEO (2000) [2] for stiff cohesive material.
The development of the p-y curve using Matlock (1970) consists of calculating the intimate resistance value p_u :

$$p_u = \min \begin{cases} 3\,S_u\,D + \sigma'_v\,D + J\,S_u\,z \\ 9\,S_u D \end{cases}$$

We calculate the value of y_{50} as :

$$y_{50} = 2.5\,E_{50}\,D$$

- E_{50} = Strain at 50% maximum stress [-]

The parameters J and E50 can be selected manually. Alternatively, users can specify the clay consistency (soft, firm, stiff or hard) with the resulting parameters listed in Table 2. For stiff soil, we consider J=0.25 and E_{50}=0.005.
The p-y curves are defined as follow :

Table 20. Static and cyclic p-y curves recommended by API (2000) [2]

Static		**Cyclic**			
		$z > z_r$		**$z < z_r$**	
y/y_{50}	**p/p_u**	**y/y_{50}**	**p/p_u**	**y/y_{50}**	**p/p_u**
0.0	0.0	0.0	0.0	0.0	0.0
0.1	0.23	0.1	0.23	0.1	0.23
0.3	0.33	0.3	0.33	0.3	0.33
1.0	0.50	1.0	0.50	1.0	0.50
3.0	0.72	3.0	0.72	3.0	0.72
8.0	1.00	∞	0.72	15.0	0.72 z/z_r
∞	1.00			∞	0.72 z/z_r

An example of static and cyclic PY curves is illustrated in Figure 40.

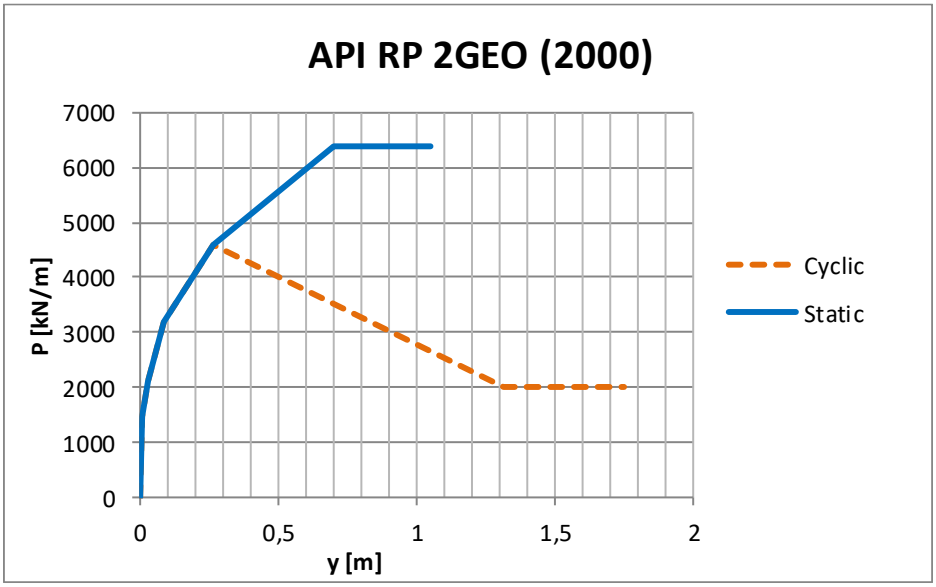

Figure 40. Static and cyclic P-Y curves (API RP 2 GEO, 2000)

11.2.4 Dunnavant (1989)

Dunnavant (1989) [7] carried out a series of full-scale, cyclic, lateral load tests on instrumented piles of varying diameter at a test site in submerged, overconsolidated clay. A p-y model is derived from the tests that defines the effect of pile diameter, relative pile-soil stiffness, and number of load cycles on the unit load-deflection relationship for soil of the type encountered at the test site. The model is particularly well-suited to large-diameter piles.
The ultimate soil resistance is calculated as :

$p_u = N_p S_u D$

$N_p = \min\left(2 + \frac{\sigma'_v}{S_a} + 0.4\frac{z}{D}, 9\right)$

- For static conditions, the Dunnavant PY curve method is calculated by:

$$p = 1.02 \cdot p_u \cdot \tanh\left[0.537\left(\frac{y}{y_{50}}\right)^{0.7}\right] \text{ for } y<8y_{50}$$

where

- $y_{50} = 0.0063 \cdot E_{50} \cdot D \cdot K_R^{-0.875}$
- K_R = the relative soil-pile stiffness and is included as a parameter to account for elastic coupling of the p-y curves. And is equal to EI/E_sL^4. K_R might typically be 0.001.

- For cyclic conditions, the determination of p-y curve is done using the following formulations:

The initial part of the p-y cyclic curve is the same as static p-y curve, until $y = y_{cm}$.

$$y_{cm} = 1m10^{\left[\frac{\log\left[\left(\frac{y_{50}}{1m}\right)^{0.7}\right] \cdot \frac{\tanh^{-1}\left(\frac{0.98p_{cm}}{p_u}\right)}{0.537}}{0.7}\right]}$$

Where

$p_{cm} = N_{cm} S_u D$ the peak value of soil resistance in cyclic loading

$p_u = N_p S_u D$ the soil resistance in static loading

- $N_{cm} = N_p \cdot \min\left[1 - \left(0.45 - 0.18\frac{z}{z_0}\right) \cdot \log(N), 1\right]$
- $N_p = \min\left(2 + \frac{\sigma'_v}{S_a} + 0.4\frac{z}{D}, 9\right)$
- N is the number of loading cycles, typically 100 to 200
    - For $y \le y_{cm}$: $p = 1.02 \cdot p_u \cdot \tanh\left[0.537\left(\frac{y}{y_{50}}\right)^{0.7}\right]$
    - For $y \ge 12\ y_{50}$ we reach the residual part of the curve where:
      $p = p_r = p_{cm} \cdot \min\left[1 - \left(0.25 - 0.07\frac{z}{z_0}\right) \cdot \log(N), 1\right]$
    - For $y_{cm} \le y \le 12y_{50}$, the first and the last part of the curve are linearly connected.

The overall shape of the curve is shown in the figure below:

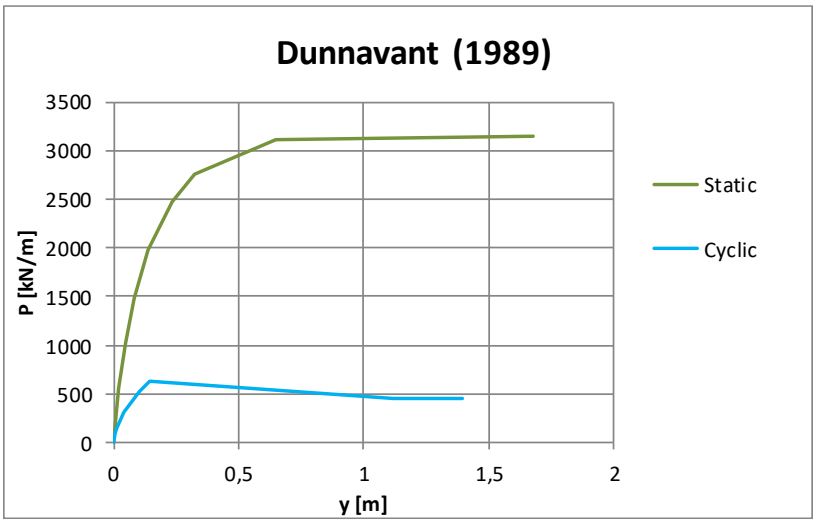

Figure 41. Typical p-y curve for cyclic loading (Dunnavant (1989))

11.2.5 Modified Matlock (1979)

The Modified Matlock (1979) [10] method was proposed by Fugro (1979) to construct p-y curves for stiff clays subjected to cyclic loading. The advantage of this method is the modelling of rapid degradation of lateral resistance of stiff clays under cyclic loading and the reduction of maximum soil resistance under cyclic loading.

This model can replace the Reese 1 al. (1975) [29] model in the case of soils without significant secondary structure (fissures, joints and slickensides) and E_{50} values of about 2% (for undrained shear strength of about 200 kPa).

The Modified Matlock (1979) approach modifies the cyclic curves p-y of the classical Matlock (1970) method only at shallow depths (i.e. above the critical length). The modifications are presented in Table 21.

We start by developing the p-y curve using Matlock (1970) [20] and calculating the intimate resistance value p_u:

$$p_u = \min \begin{cases} 3\,S_u\,D + \sigma'vD + J\,S_u\,z \\ 9\,S_u D \end{cases}$$

The parameters J and E_{50} can be selected manually. Alternatively, users can specify the clay consistency (soft, firm, stiff or hard) with the resulting parameters listed in Table 19. For stiff soil, we consider J=0.25 and E_{50}=0.005.

Table 21. Cyclic p-y coordinates for stiff cohesive soil (Modified Matlock (1979)[10])

Point	Cyclic	
	y/y_c	**p/p_u**
1	0.1	0.23
2	0.3	0.34
3	1.0	0.50
4	15.0	0.72 z/X_r

* $X_r = 6\,S_u\,D / (\gamma'D+J\,S_u)$

$y_{50} = 2.5\,E_{50}\,D$

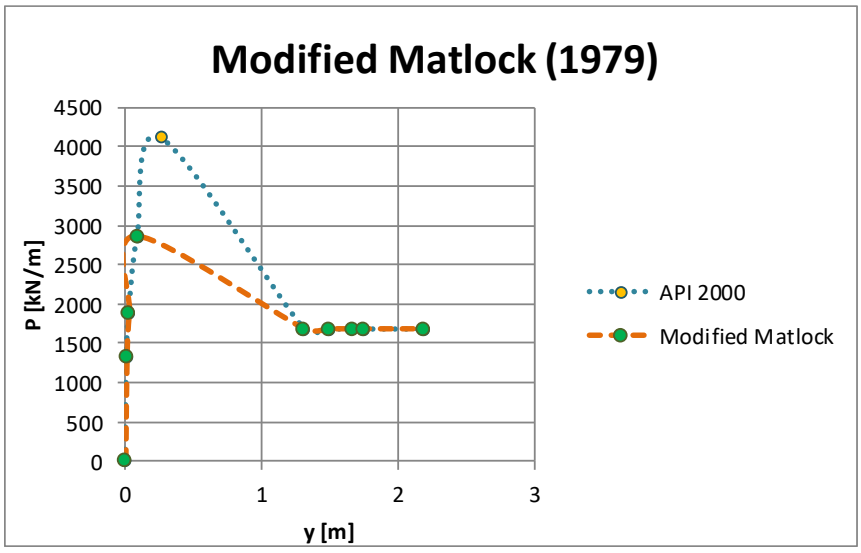

Figure 42. Typical p-y data in stiff cohesive material under cyclic loading - Modified Matlock (1979) vs Matlock (1970)

11.3 Frictional soil

11.3.1 O'Neil and Murchison (1983) - API RP2GEO (2011)

The API RP2GEO (2011) [3] model is based on the O'Neil and Murchison (1983) [23] tangent hyperbolic method.
The ultimate resistance is calculated as

$$p_u = \min \begin{cases} (C_1\, z + C_2\, D)\sigma'_v \\ C_3\, D\, \sigma'_v \end{cases}$$

Where:

- C_1, C_2 and C_3 = Coefficients depending on the soil effective angle of internal friction

$$C_1 = \frac{\tan^2\beta \tan\alpha}{\tan(\beta-\varphi)} + K_0\left(\frac{\tan\varphi \sin\beta}{\cos\alpha \tan(\beta-\varphi)} + \tan\beta\,(\tan\varphi \sin\beta - \tan\alpha)\right)$$

$$C_2 = \frac{\tan\beta}{\tan(\beta-\varphi)} - K_a$$

$$C_3 = K_a(\tan^8\beta - 1) + K_0 \tan\varphi \tan^4\beta$$

Where :

- φ : friction angle [°]
- K_0 is the coefficient of earth pressure at rest, it can be defined by the user or take a value of 0.4 as recommended by API.
- $\alpha = \varphi/2$,
- $\beta = 45 + \varphi/2$,
- K_a = Rankine minimum active earth pressure coefficient =(1 - sin φ)/(1 + sin φ) or user-defined

The curve is defined as:

$$p = A \cdot p_u \cdot \tanh\left(\frac{k \cdot z}{A \cdot p_u} \cdot y\right) p \le p_u$$

where

- k is the rate of increase with depth of the initial modulus of subgrade reaction [kPa/m] and can be approximated by the following equation :
  k = max(197.8 φ'^{2}-10232 φ + 136820 ; 5400 kPa) or user-defined

- A= max $\begin{cases} 3 - 0.8\, z/D \\ 0.9 \end{cases}$ for static loading and 0.9 for cyclic loading

The development of the p-y curve of a frictional soil following O'Neil and Murchison (1983) method is presented in Figure 13.

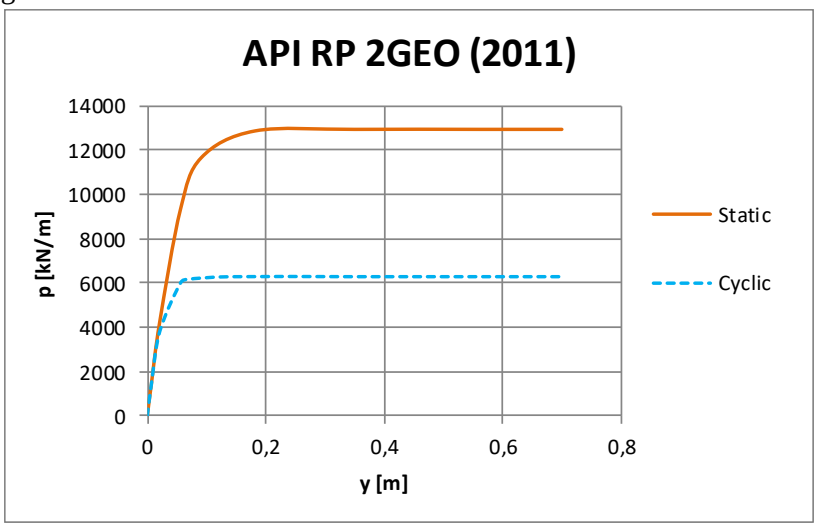

Figure 43. Typical p-y curves in frictional soil following O'Neill and Murchison (1983) method

11.3.2 O'Neil and Murchison (1983)modified by KALLEHAVE & al. (2012)

Kallehave et al (2012) [14] method is based on the API RP 2GEO (2011) [3]approach but is modified in order to be adapted to large diameter piles specifically used in the offshore wind turbine foundations in sand. The proposed modification consists of changing the rate increase of the modulus of subgrade reaction with depth k [kPa/m] as follow :

$$E_{mod} = k \cdot z_0 \cdot \left(\frac{z}{z_0}\right)^m \cdot \left(\frac{D}{D_0}\right)^{0.5}$$

Where

- z_0 = Reference depth = 2.5 m
- D_0 = Reference diameter = 0.61 m
- m = 0.6

Finally, the PY curve is calculated as :

- for $p \leq p_u$: $p = A \cdot p_u \cdot \tanh\left(\frac{E_{mod}}{A \cdot p_u} \cdot y\right)$

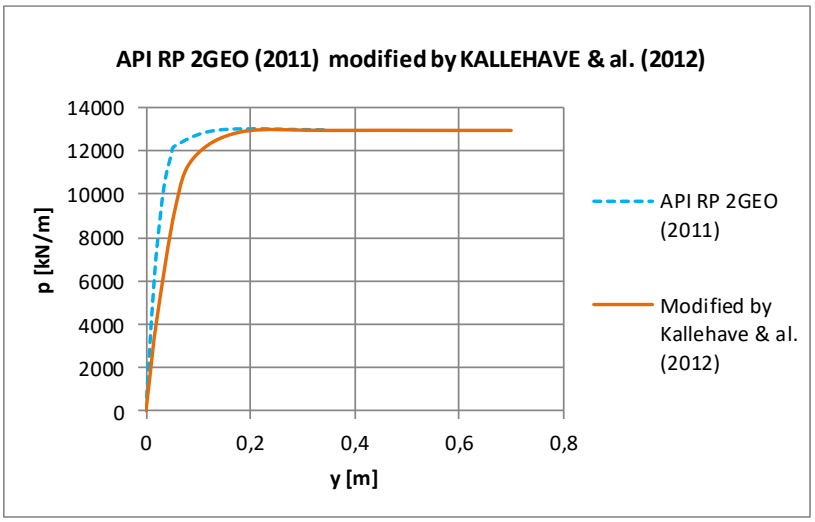

Figure 44. P-Y curve modified by Kallehave & al. (2012)

11.3.3 O'Neil and Murchison (1983)modified by SORENSEN & al. (2010)

Sorensen et al (2010) [30] method is based on the API RP 2GEO (2011) [3] approach but is modified in order to be adapted to monopoles with diameters of 4 to 6 m in sand. The proposed modification consists of changing the rate increase of the modulus of subgrade reaction with depth k [kPa/m] as follow :

$$E_{mod} = a \cdot \left(\frac{z}{z_0}\right)^b \cdot \left(\frac{D}{D_0}\right)^c \varphi^d$$

Where

- z_0 = Reference depth = 1.0 m
- D_0 = Reference diameter = 1.0 m
- a = 50000 kN/m^2
- b = 0.6
- c = 0.5
- d = 3.6

Finally, the PY curve is calculated as :

- for $p \leq p_u$: $p = A \cdot p_u \cdot \tanh\left(\frac{E_{mod}}{A \cdot p_u} \cdot y\right)$

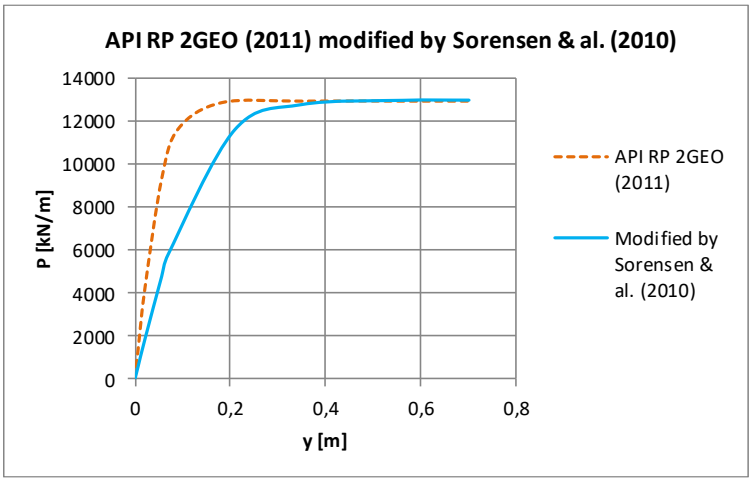

Figure 45. P-Y curve modified by Sorensen & al. (2010)

11.3.4 Wesselink (1988)

Wesselink et al. (1988) [36] recommendations can be used in the case of calcareous sand. The determination of p-y curve is done using the following equation for static and cyclic loading:

$$p(y) = R \cdot D \cdot \left(\frac{z}{z_0}\right)^N \cdot \left(\frac{y}{D}\right)^\gamma \leq p_u$$

Where:

- R = control variable for curve stiffness [kPa]
- N = constant controlling the rate of increase in p with depth z
- z_0 = Specified constant depth = 1 m [m]
- γ = is the soil unit weight [kN/m^3]

Typical values of the input parameters for offshore piles are shown below:

Table 22. Typical values of input parameters

Reference	Soil Test and Type	R [kPa]	N	γ
Wesselink et al (1988)	Bass Strait, Kingfish B centrifuge tests	650	0.7	0.65
Wesselink et al (1988)	Bass Strait, Halibut centrifuge tests	850	0.7	0.65

The ultimate soil resistance is calculated as follow:

$p_u = K_p^2 \, \sigma'_{v0} \, D$

Where:

- K_p = Coefficient of passive earth pressure [-] = (1+sin(φ'))/(1-sin(φ')) or user-defined

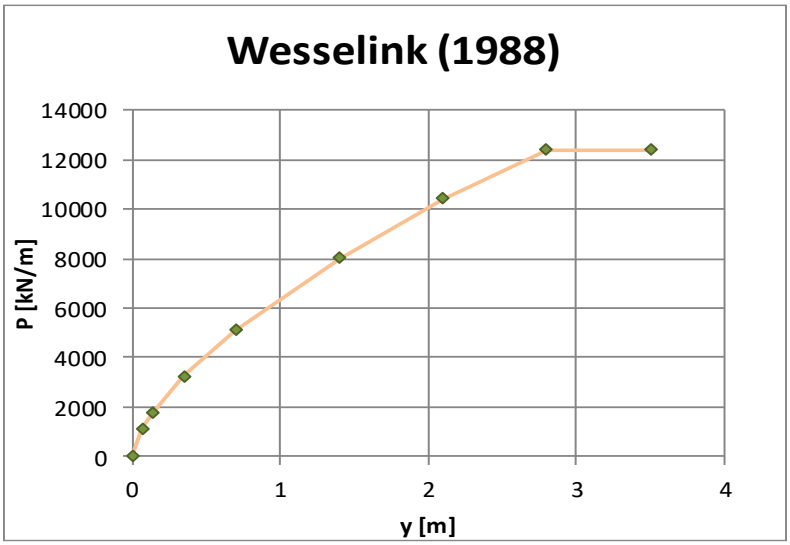

Figure 46. p-y data (Wesselink et al. (1988))

11.3.5 Dyson & Randolph (2001)

Dyson & Randolph (2001) [8, 9] developed p-y static curves for carbonate sands based on the results of a series of model centrifuge tests. The p-y curves were formed in terms of CPT q_c measurements as follow

$$p(y) = \gamma' \cdot D^2 \cdot R \left(\frac{q_{net}}{\gamma \cdot D}\right)^n \cdot \left(\frac{y}{D}\right)^m$$

where

- q_{net} = net cone resistance [kPa]
- R = control coefficient for curve stiffness. It takes values between 2.56 and 2.84

- N = constant controlling the rate of increase in p with depth z. Typical value N= 0.7
- γ = is the soil unit weight. Typical value γ = 0.65 kN/m^3
- n=0.72
- m = constant controlling the amount of curvature in the p-y relation. It takes values between 0.52 and 0.64

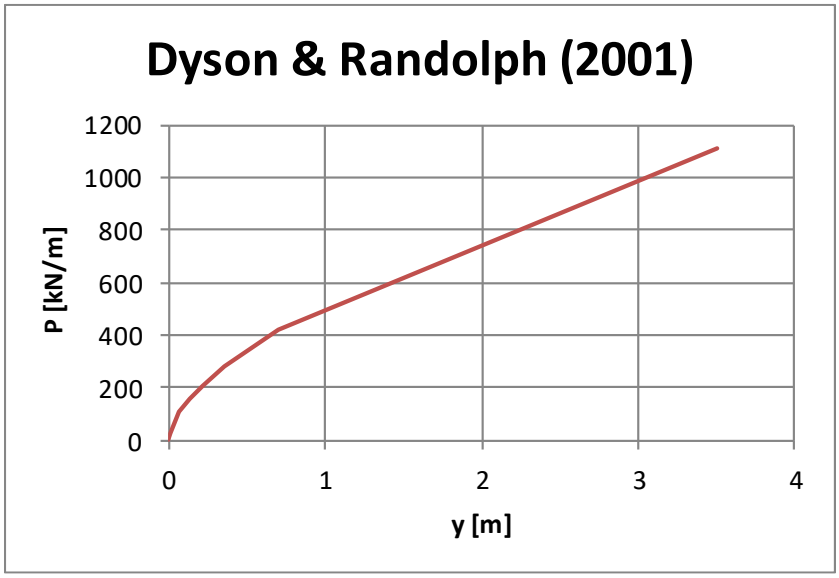

Figure 47. P-Y (static) curve given by Dyson & Randolph (2001)

11.3.6 Novello (1999)

Novello (1999) [22] developed a method to define static PY curves for use in uncemented or very weakly cemented calcareous sediments based on CPT measurements :

$$p = 2D(\sigma'_v)^{0.33}(q_{net})^{0.67}\left(\frac{y}{D}\right)^{0.5} < p_u = q_{net} \cdot D$$

where q_{net} = net cone resistance [kPa]

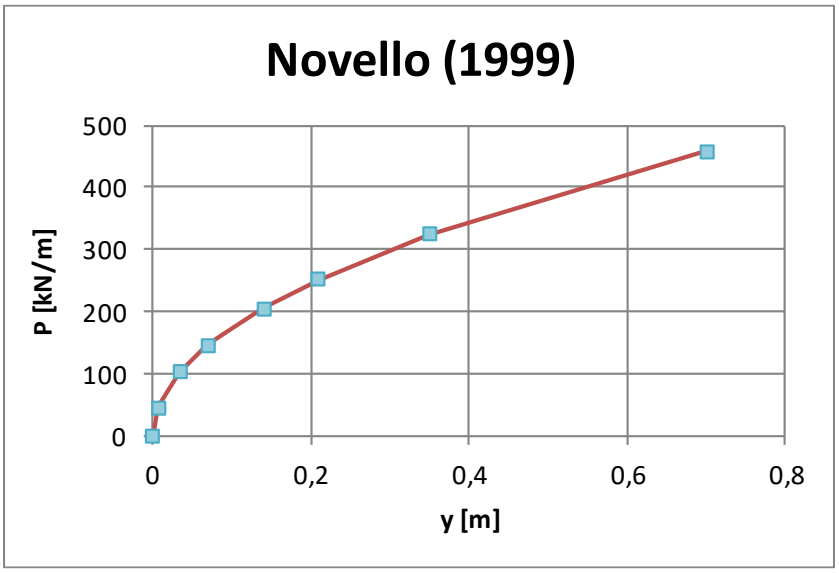

Figure 48. P-Y (static) curve given by Novello (1999)

11.3.7 SOLCYP (2017)

The SOLCYP project [25] provides accurate results for the case of cyclic loading, taking into account various parameters that are demonstrated to be important for the system behavior under cyclic conditions. The approach is explained in detail in paragraph 5.2.
In the case of cohesion-less soils of medium to high density (I_D greater than 50%), the local SOLCYP method is tenting to take into account the soil-pile interactions during cyclic loading by reaction p-y curves deduced from the static p-y curves (for any available static approach) by application of appropriate reduction factors. Table 23 presents the values of P-multipliers r_c that have to be applied at each depth.

Table 23. Case of sands of medium or high density – Expression of coefficients r_c (P-multipliers) to be applied to the reaction P of the static P-y curves [25]

Relative depth	z/D from 0 to 1.5	z/D from 1.5 to 3	z/D from 3 to 5	z/D > 5
Multipliers r_c	$(1-4R_1)(1+4R_2)$	$(1-2R_1)(1+2R_2)$	$(1-R_1)(1+R_2)$	1

Where $R_1 = \left[\log(N) + 3\frac{H_c}{H_{max}}\right]/20$ and $R_2 = 2.5 \cdot \left[1 - 2\frac{H_{max}}{H_{lim}}\right]/100$

All these expressions of valuable if the maximum load H_{max} applied to the head of the pile does not exceed limit load H_{lim}.
The following figure presents an example of cyclic SOLCYP curve while the static Matlock (1970) approach is selected.

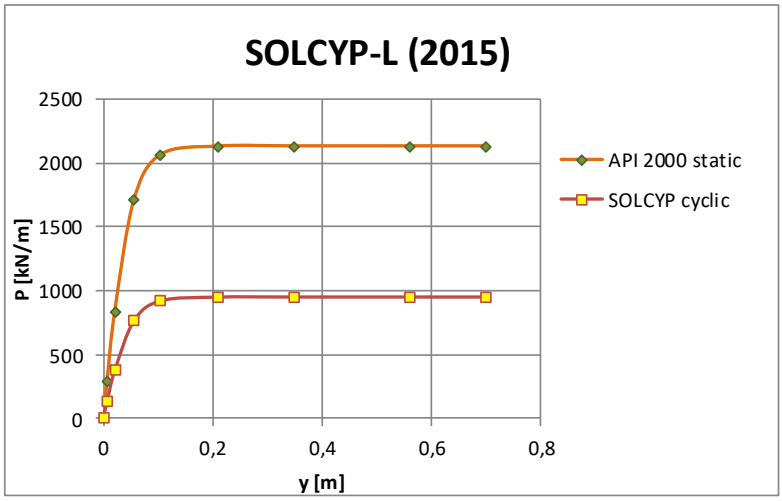

Figure 49. Example of p-y static curve degraded using SOLCYP (local) recommendations

11.4 Weak Rocks

11.4.1 Reese (1997)

The shape of weak rock p-y curve is based on Reese (1997) [27] and is made up of three sections. For the design of piles under lateral loading in rock, special emphasis is necessary in the coring of the rock. The input parameters required for this method are,

- UCS: uniaxial compressive strength [kPa],
- α_r : the rock quality designation (percent of recovery - strength reduction factor) [-]
  or RQD= Rock Quality Designation → αr = 1−2/3 (RQD%)/(100%)

- k_{rm} : a strain factor ranging from 0.0005 to 0.00005.
- E_{ir}: intact modulus of rock [kPa]
  It can be user-defined or calculated by the following expression :$E_{ir} = MR \cdot UCS$ where MR = modulus ratio [-]

In order to determine the exact value of k_{rm}, we have to examine the stress-strain curve of the rock sample. Typically, the k_{rm} is taken as the strain at 50% of the maximum strength of the core sample. Because limited experimental data are available for weak rock during the derivation of the p-y criteria, the k_{rm} from a particular site may not be in the range between 0.0005 and 0.00005. For such cases, we lay use the upper bound value (0.0005) to get a larger value of y_{rm} which in turn results in the softest p-y curves and provides a more conservative result.
The development of the p-y curve for weak rock is presented in Figure 14 (static and cyclic case). The ultimate resistance for rock, p_{ur}, is calculated from the input parameters. The linear portion of the curve with slope K_{ir} defines the curve until intersection with the curved portion defined in the figure.

$$p_u = \min \begin{cases} \alpha_r \cdot UCS \cdot D\left(1 + 1.4\,\frac{z_r}{D}\right) & , 0 \le z_r \le 3D \\ 5.2 \cdot \alpha_r \cdot UCS \cdot D & , z_r \ge 3D \end{cases}$$

The PY curve is defined as follow :

- $p = \min\left[\frac{p_u}{2}\left(\frac{y}{y_{rm}}\right)^{1/4}, K_{ir}y\right]$, if $y < 16y_{rm}$
- $p = p_u$ otherwise

Where

- $K_{ir}$is the initial stiffness, given by $K_{ir} = E_{ir} \cdot k_{ir}$
- k_{ir} is a dimensionless coefficient that accounts for changes in and is given by:
  - $k_{ir} = \begin{cases} 100 + 400 \cdot \frac{z_r}{3D} & \text{if } 0 < z_r < 3D \\ 500 \text{ otherwise} \end{cases}$
- y_{rm} is the limiting displacement for this initial elastic portion and is given by: $y_{rm} = k_{rm}D$

The p-y curve for static and cyclic conditions is given by:

- $p = \min\left[\frac{p_u}{2}\left(\frac{y}{y_{rm}}\right)^{1/4}, K_{ir}y\right]$, if $y < 16y_{rm}$
- $p = p_u$ otherwise

The general form of the p-y curve of Reese (1997) is presented in the figure bellow:

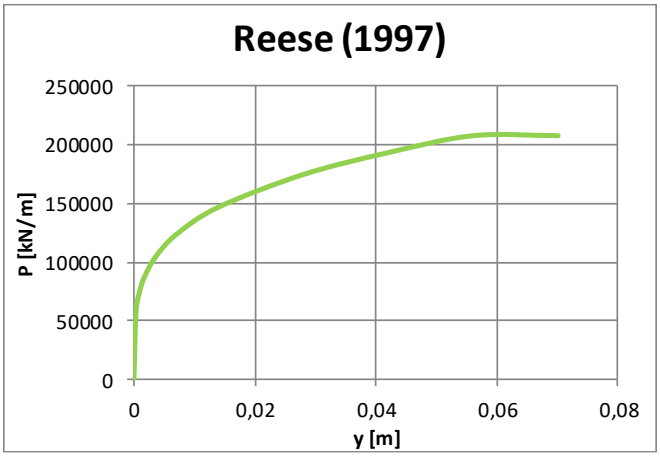

Figure 50. p-y curve for Weak Rock (Reese (1997))

11.4.2 Abbs (1983)

The ABBS method was designed for application in soft rock and is described by Abbs (1983) [1]. It was developed for carbonate rocks having strengths in the range of 0.5 to 5MPa and uses a stiff clay method as the initial part of the curve, then a sand method for the residual pressure at larger displacements.
The first part of the curve is given by the Reese et al.(1975) method for static loading in stiff clay, up until the end of the second parabolic section (i.e. y <= $6Ay_c$). After that the pressure undergoes a rapid change to the residual pressure given by the API method for sand under cyclic loading.
The PY curve is generated using the following logic:

- S_a = average shear strength over the depth z in stiff clay: $S_a = (S_u(z=0) + S_u(z))/2$
- We calculate the ultimate resistance in stiff clay $p_{u,clay} = \min \begin{cases} 2\,S_a\,D + \sigma'_v\,D + 2.83\,S_a\,z \\ 11\,S_u\,D \end{cases}$
- Constant A_{clay} for static loading in stiff clay :
- for $\frac{z}{D} \leq 3$: $A_{clay} = \min\left[-0.05\left(\frac{z}{D}\right)^2 + 0.29\frac{z}{D} + 0.2\,;0.6\right]$
  for $\frac{z}{D} > 3$: A_{clay} =0.6
- $y_{50}= E_{50}\cdot D$
- $\alpha = \varphi/2$
- $\beta = 45 + \varphi/2$
- $C_1 = \frac{\tan^2\beta\,\tan\alpha}{\tan(\beta-\varphi)} + K_0\left(\frac{\tan\varphi\tan\beta}{\cos\alpha\tan(\beta-\varphi)} + \tan\beta\,(\tan\varphi\sin\beta - \tan\alpha)\right)$
- $C_2 = \frac{\tan\beta}{\tan(\beta-\varphi)} - K_a$
- $C_3 = K_a(\tan^8\beta - 1) + K_0\tan\varphi\tan^4\beta$
- Ultimate resistance in sand $p_{u,sand} = \min \begin{cases} (C_1\,z + C_2\,D)\sigma'_v \\ C_3\,D\,\sigma'_v \end{cases}$
- A_{sand} = dimensionless constant for cyclic loading in sand : A_s= 0.9
- k_{sand} = rate increase of the modulus of subgrade reaction in sand [kPa/m]
  Estimated by the following equation $k_s = \max(197.8\varphi'^2 - 10232\varphi' + 136820\ ;\ 5400\ \text{kPa})$
- k_{clay} = Rate of increase with depth of the initial modulus of subgrade reaction <u>in stiff clay</u> [kN/m3]
  It can be user-defined or calculated as follow :
  - if $50 \leq S_a \leq 100$ ⇨ k =$135\cdot10^3$ kN/m^3
  - if $200 \leq S_a \leq 300$ ⇨ k =$270\cdot10^3$ kN/m^3
  - if $300 \leq S_a \leq 400$ ⇨ k =$540\cdot10^3$ kN/m^3
- K_0 = coefficient of earth pressure [-]
  K_0 = 0.4 **!** or User defined
- K_a = Rankine minimum active earth pressure coefficient
  K_a = (1 - sin φ)/(1 + sin φ) or user-defined

The PY curve is defined as follow :

- For $y \leq A_{clay}\,y_{50}$: $p = \min\left(k_{clay}\,z\,y\ ;\ \frac{p_{u,clay}}{2}\sqrt{\frac{y}{y_{50}}}\right)$
- For $A_{clay}\,y_{50} < y \leq 6\,A_{clay}\,y_{50}$:
  $p = \frac{p_u}{2}\sqrt{\frac{y}{y_{50}}} - 0.055p_{u,clay}\left(\frac{y - A_{clay}\,y_{50}}{A_{clay}\,y_{50}}\right)^{1.25}$

- For $y \geq 6A_{clay}y_{50}$: $p = A_{sand} \cdot p_{u,sand} \cdot \tanh\left(\frac{k_{sand} \cdot z}{A_{sand} \cdot p_{u,sand}} \cdot y\right)$

The method does not vary for static and cyclic loading.

Typical curves for the ABBS method are shown below:

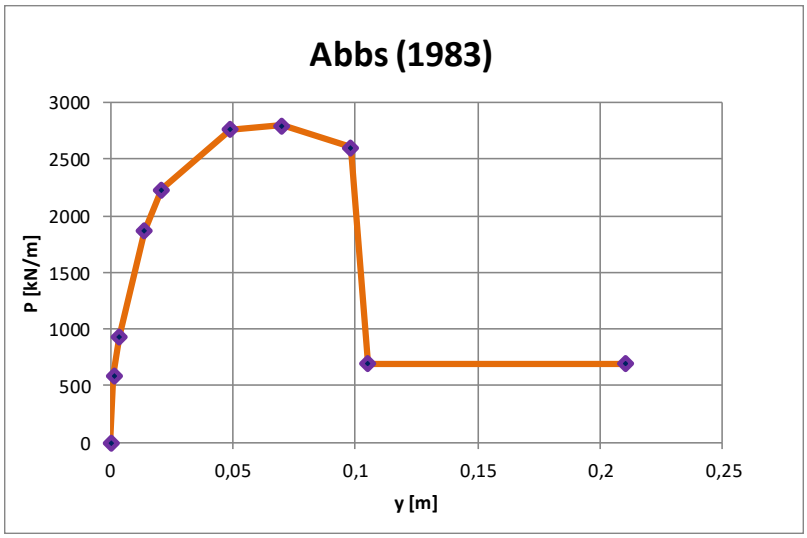

Figure 51. Typical curves for the ABBS method